ALTERED CALCIUM SIGNALING IN THE GRANULE CELL LAYER OF ATAXIC MUTANT MICE

By

Matthew G. Lamont

A Thesis submitted to the

School of Graduate Studies

In partial fulfillment of the requirements for the degree of

Masters of Science (Neuroscience)

Faculty of Medicine

Memorial University of Newfoundland

May 2014

St. John's Newfoundland

Abstract

The waddles mouse is characterized by a namesake waddling "side-to-side" gait, which is the result of a deficiency in the enzyme carbonic anhydrase type 8 known to inhibit the binding of inositol 1,4,5-trisphosphate to receptors on intracellular calcium stores. Behavioral experiments were conducted utilizing a rota-rod apparatus to further characterize this ataxia. The results indicated the homozygotes performed significantly worse than heterozygotes or wild type animals, and that younger homozygotes outperformed older cohorts. To elucidate potential alterations in cellular calcium signaling, acute cerebellar slices from the vermis were harvested for calcium imaging experiments *in vitro*. These experiments revealed significant alterations in granule cell somatic calcium signaling in waddles mice. I propose that cerebellar calcium signalling is altered in waddles mice, and that these alterations may be contributing to the observed ataxia through developmental mechanisms. These results will aid in understanding ataxias whose pathological basis involves alterations in neuronal calcium signaling.

Acknowledgments

I would like to thank my supervisor, Dr. John Weber, for his continued advice and support both in conducting experiments for and the writing of this thesis. I would also like to thank my other supervisory committee members, Drs. Michiru Hirasawa & Qi Yuan, for their helpful comments and technical advice. Lastly, but not least; thanks to my family and friends who have supported me before, during, and after this work.

This work was supported by grants from the Natural Sciences and Engineering Research Council (NSERC), and the Canada Foundation for Innovation (CFI).

Table of Contents

List of Figures

List of Abbreviations

α-CaMKII – α-Ca^{2+}/Calmodulin-Dependant Protein Kinase II

aCSF – Artificial Cerebrospinal Fluid

AIDA - 1-Aminoindan-1,5-Dicarboxylic Acid

AMPA - α-Amino-3-Hydroxy-5-Methyl-4-Isoxazolepropionate

ARR – Accelerating Rota-Rod

AUTC – Area-Under-The-Curve

Ca^{2+} - Ionic Calcium

$CaCl_2$ – Calcium Chloride

cAMP - Cyclic Adenosine Monophosphate

CaN - Calcineurin

CAR8 – Carbonic Anhydrase Type 8

CCD – Charge Coupled Device

CF – Climbing Fiber

CIF – Calcium Influx Factor

CO_2 - Carbon Dioxide

CoV – Coefficient of Variation

CNQX - 6-Cyano-7-Nitroquinoxaline-2,3-Dione

CNS – Central Nervous System

DAG - Diacylglycerol

DHPG - (S)-3,5 Dihydroxyphenylglycine

EPSC - Excitatory Post-Synaptic Current

EPSP – Excitatory Post-Synaptic Potential

ER – Endoplasmic Reticulum

GABA - Gamma-Aminobutyric Acid

GoC – Golgi Cell

GC – Granule Cell

GCL – Granule Cell Layer

Hz - Hertz

IP_3 - Inositol 1,4,5-trisphosphate

IPSC – Inhibitory Post-Synaptic Current

KCl – Potassium Chloride

LTD – Long Term Depression

LTP – Long Term Potentiation

MF – Mossy Fiber

$MgSO_4$ – Magnesium Sulfate

ML – Molecular Layer

Mo. - Month

mGluR – Metabotropic Glutamate Receptor

NaCl – Sodium Chloride

$NaHCO_3$ – Sodium Bicarbonate

Na_2HPO_4 – Sodium Phosphate Dibasic

NMDA - *N*-Methyl-D-Asparate

O_2 - Oxygen

OG-BAPTA-1-AM – Oregon Green 488 BAPTA-1AM

PC – Purkinje Cell

PF – Parallel Fiber

PI – Propidium Iodide

PIP2 - Phosphatidylinositol 4,5 Bisphosphate

PLC – Phospholipase C

PKC – Protein Kinase C

PNA – Postnatal Age

PP2B - Protein-Phosphatase-2B

PrP^C - Cellular Prion Protein

ROI – Region of Interest

RORα – Retinoid-Related Orphan Receptor α

R.P.M. – Rotations Per-Minute

RyR – Ryanodine Receptor

SERCA - Sarcoplasmic-Endoplasmic Reticulum Calcium-ATPase

SEM – Standard Error of the Mean

SMOC - Second Messenger-Operated Channel

SOC - Store-Operated Channel

TRP(C) - Transient Receptor Potential (Canonical)

VGCC – Voltage Gated Calcium Channel

VOR - Vestibulo-Ocular Reflex

Wdl – Waddles

WT – Wild Type

$[Ca^{2+}]_i$ – Intracellular Calcium Concentration

Chapter 1 Introduction

1.1 General

Motor coordination and learning are the primary responsibilities of the cerebellum; the cellular basis of which heavily involves the plastic ability of various synapses (Ito, 2006). Damage to the cerebellum often leads to symptoms such as ataxia, asynergy, dysmetria, and motor learning deficits in humans (Schmahmann, 2004; Stoodley & Schmahmann, 2010) as well as in other mammalian species such as rabbits or various rodents (Lalonde & Strazielle, 2001; Rinaldo & Hansel, 2010). Cerebellar dysfunction can be due to acute changes in cellular physiology causing a direct effect (i.e. an altered intracellular concentration of calcium in neurons; Zagha et al., 2010), or to changes caused indirectly by chronic changes in cerebellar physiology (i.e. an altered intracellular calcium concentration, over time, causes changes to cellular morphology in the cerebellar cortex; Lalonde & Strazielle, 2001). The mutant waddles (*wdl*) mouse is an excellent model to study how a change in cerebellar physiology, specifically physiology involving calcium (Ca^{2+}) signaling, affects cerebellar development and ultimately motor output. This is because of a mutation affecting intracellular Ca^{2+} signaling that is localized, within the central nervous system (CNS), to the cerebellum alone.

The *wdl* mouse is a spontaneous mutant which exhibits a wobbly side-to-side gait and appendicular dystonia as an ataxic phenotype (Jiao et al., 2005). Genotyping of this mutant revealed a 19-bp deletion in the gene encoding for carbonic anhydrase type 8 (CAR8; Jiao et al., 2005). The deletion causes a virtual absence of functional CAR8 in homozygous animals which display a phenotypic ataxia. Interestingly, heterozygous

animals with only one faulty copy of the gene, and therefore about half of the functional copies of CAR8 see in non-mutated animals theoretically, retain their motor skillfulness. CAR8 has been shown previously to reduce the release probability of Ca^{2+} from intracellular stores by inhibiting the binding of inositol 1,4,5-trisphosphate (IP_3) to its receptor (inositol 1,4,5-trisphosphate receptor; IP_3R). It is expressed primarily in the cerebellum of mice with particularly high localization in the molecular layer (ML) and peri-somatically in Purkinje cells (PC; Yan et al., 2007; Aspatwar, et al., 2010). The IP_3R is located intracellularly on the endoplasmic reticulum (ER) and controls the release of Ca^{2+} from internal stores.

As the homozygous *wdl* mice lack functional CAR8, we would expect to see more Ca^{2+} released in the cerebellum of these animals in response to stimulation affecting the IP_3 signaling pathway in neurons. The major goal of this study is to determine if the hypothesized alteration in neuronal Ca^{2+} response is indeed present in the cerebellum of *wdl* mice, and also to characterize these differences; both between heterozygous and homozygous *wdl* mutants, as well as between *wdl* mutants and wild type (WT) animals. These important concepts and more are discussed further and with more detail in subsequent sections.

1.2 The Cerebellum

The cerebellum is involved in fine tuning motor output by controlling aspects such as balance, smoothness of movements, and gait (Ito, 2006). The cerebellum achieves this by processing a large amount of afferent converging information from areas such as the

vestibular nuclei and inferior olive complex into a relatively small amount of efferent information. This outgoing signal is conducted by the sole output neuron of the cerebellar cortex, the PC (Ito, 2006). PC output is mediated by the chief inhibitory neurotransmitter of the mammalian nervous system, gamma-aminobutyric acid (GABA). GABAergic output of the PCs inhibits deep cerebellar and vestibular nuclei, modulating cerebral motor commands as they are propagated towards the spinal cord. Before the output signal leaves the cerebellum, there is an enormous amount of internal processing that occurs within the cerebellar circuitry. The first step in the cerebellar circuitry is incoming mossy fibers (MFs) that originate from numerous sources in the peripheral nerves, spinal cord, and brain stem, synapsing onto 400-600 granule cells (GC). Each of these GCs then projects their axon as parallel fibers (PFs) which each synapse with as many as 300 PCs (Eccles et al., 1967). Along all of these connections there are also several types of inhibitory interneurons modulating the afferent signal, further complicating this neuronal circuitry (Fig. 1.1). Specific interactions between various neuronal types and projections are discussed below.

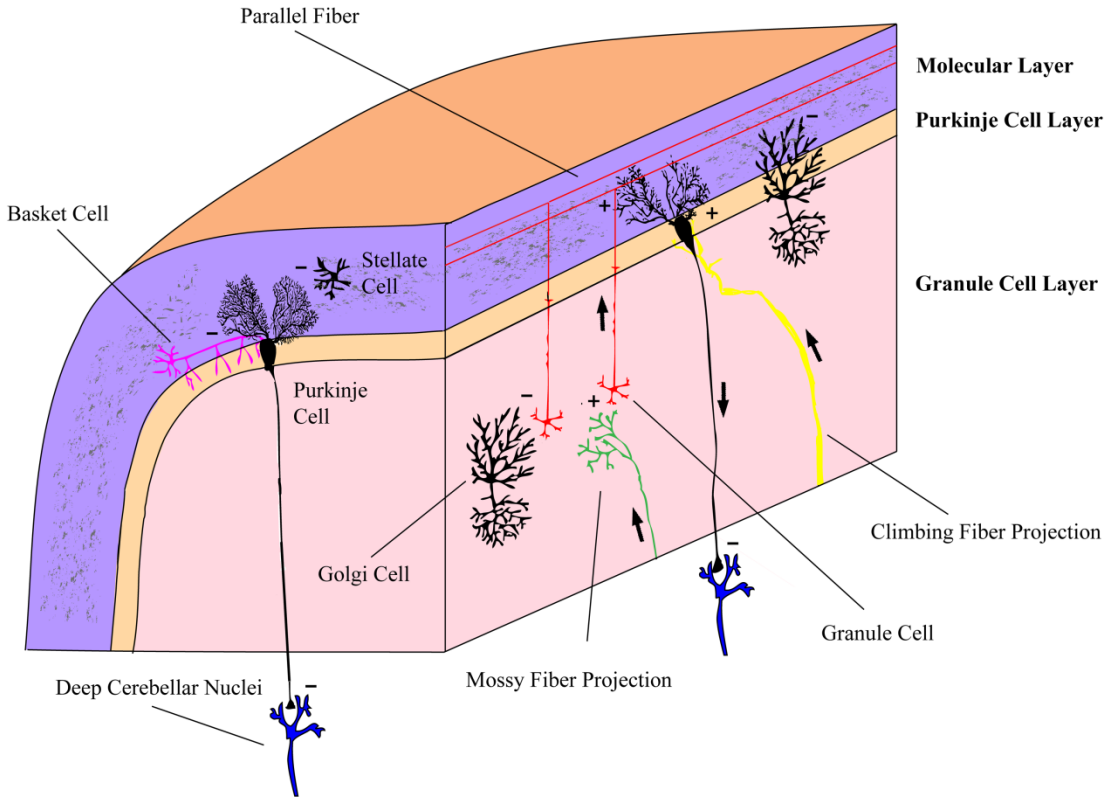

Figure 1.1 - Neurons and circuits of the cerebellum – The main signaling circuit of the cerebellum begins with an incoming stimulus from the mossy fiber (MF; Green), a projection from precerebellar nuclei (e.g. vestibular nuclei, reticular nuclei). The MF forms an excitatory synapse with granule cells (GCs; Red) that is also modulated by Golgi cell (GoC; Black) inhibitory input. When excited the GCs stimulate PCs (Black) via the GC projections called parallel fibers (PFs; Red), which can also be inhibited by neighbouring GoCs. However, the PCs excitability is further modulated by several other types of cells. The inhibitory interneurons (Basket and Stellate cells, magenta/black respectively) are located in the ML and provide inhibitory input. PCs receive additional excitatory input from CFs (Yellow) which originates in the inferior olivary complex. Based on the temporal and spatial summation of all incoming signals, the PCs will either continue their tonic inhibition of the deep cerebellar nuclei (Blue) or the inhibition will be temporarily attenuated; generally this is either a result of or will modulate motor behaviour and/or motor learning based in the cerebellum.

1.3 The Importance of Calcium in the Cerebellum

Calcium, in its ionic form, is present throughout the nervous system and carries out a variety of important roles. Ca^{2+} is necessary for proper neuronal growth and development, neurotransmission throughout the central and peripheral nervous system, and can lead to differential patterns of gene expression (Lamont & Weber, 2012). Calcium is also required for several forms of synaptic plasticity in the hippocampus, cerebral cortex, and cerebellum (Bliss & Collingridge, 1993; Malenka & Nicoll, 1999; Rose & Konnerth, 2001). Synaptic plasticity is the ability of either the presynaptic or postsynaptic neuron of a given synapse to either modify the strength of signal released or to respond to a signal more effectively, respectively (Collingridge, 1990). It is theorized that by modifying how strongly a synapse will respond to stimulation, our neural network is encoding salient information from our environment. Long-term depression (LTD), particularly at PF-PC synapses in the cerebellum, is the widely accepted vertebrate model for a cellular mechanism that underlies synaptic changes during motor learning and memory formation in the cerebellum. LTD is said to occur at a synapse when there is activity-dependant reduction in the efficiency of the synapse, which can be due to both pre- and post-synaptic changes. Several molecular components have been identified which appear to be necessary for its induction, including glutamate receptors and various kinases (Massey & Bashir, 2007). It was long thought that PF-PC synapses were the only synapses capable of plasticity in the cerebellar cortex, however in recent years plasticity has been described at several other synapses (Hansel et al., 2001; Dean et al., 2010).

In the cerebellum the excitability and signaling in neurons is highly tied to the excitatory glutamatergic neurotransmitter system. Glutamate activates two main receptor types in cerebellar neurons, the ionotropic AMPA, Kainate, and NMDA receptors; and the metabotropic glutamate receptor family.

Ionotropic receptors allow Ca^{2+} influx either directly through their channel when activated by glutamate, or indirectly by contributing to membrane depolarization which affects voltage-gated Ca^{2+} channels (VGCCs). NMDA receptors are well distributed in the brain and were only recently described in adult PCs (Piochon et al., 2007; Renzi et al., 2007). Activation of this receptor subtype primarily causes an influx of Ca^{2+} into the cell. Alternatively, AMPA and kainate receptor activation leads primarily to sodium influx. Although some types of these receptors can also be permeable to Ca^{2+} depending on their subunit combination. AMPA receptors containing a GluR2 subunit are Ca^{2+}–impermeable, while those lacking this subunit are permeable to Ca^{2+} (Liu & Cull-Candy, 2005). AMPA receptor activation can also indirectly lead to Ca^{2+} influx by inducing membrane depolarization activating VGCCs. Additionally, membrane depolarization increases the activation of NMDA receptors which are also sensitive to the membrane potential of the cell through their magnesium blockade.

Metabotropic glutamate receptor types are divided into three groups. Group 1 mGluRs (mGluR 1 and 5) lead to intracellular Ca^{2+} increases via a G-protein coupled to phospholipase C (PLC). PLC cleaves phosphatidylinositol 4,5 bisphosphate (PIP_2) from the cell membrane, producing diacylglycerol (DAG), which activates the enzyme protein kinase C (PKC), and IP_3, which binds to IP_3Rs on intracellular Ca^{2+} stores located on the ER, resulting in a release of Ca^{2+} from the stores and an elevation of intracellular free

Ca^{2+} (Fig. 1.2). In many types of neurons, the depletion of Ca^{2+} stores also stimulates influx of extracellular Ca^{2+} through channels on the plasma membrane, a process termed "capacitative Ca^{2+} influx" (Weber et al., 2001; Baba et al., 2003). Studies have shown that activation of group I mGluRs can enhance the elevation of Ca^{2+} mediated by NMDA receptors (Bruno et al., 1995; Rahman & Neuman, 1996). Group II (mGluR2 and 3) and III (mGluR4 & mGluR6-8) metabotropic glutamate receptors are also G-protein linked and inhibit adenylate cyclase causing lower levels of cyclic adenosine monophosphate (cAMP) and in general lower levels of intracellular Ca^{2+} (Coutinho & Knöpfel, 2002).

Some of the best understood forms of synaptic plasticity involve the PCs. LTD represents a persistent decrease of postsynaptic sensitivity to glutamate caused by the removal of AMPA receptors from the membrane via endocytosis (Ito, 2006). This endocytic mechanism is thought to be the primary method for plasticity-mediated memory encoding in PCs, as an input-specific type of synaptic plasticity. Both PF-LTD and CF-LTD on PCs are dependent on an AMPA-receptor induced membrane depolarization and subsequent Ca^{2+} influx through VGCCs (Hansel & Linden, 2000; Hansel et al., 2001). Activation of mGluRs also appears to be necessary for expression of LTD at both of these synapses, most likely via the above mentioned coupling of group I mGluRs to the IP_3 pathway (Daniel, Levenes, & Crépel, 1998; Kohda, Inoue, & Mikoshiba, 1995). PC synaptic plasticity was thought to be NMDA receptor-independent, until recently when their activation at CF-PC synapses was found necessary for PF-LTD induction (Piochon et al., 2010). In addition to large Ca^{2+} transients, PF-LTD expression is dependent on activation of the enzymes α-Ca^{2+}/calmodulin-dependant protein kinase II (α-CaMKII) and PKC (Piochon et al., 2010).

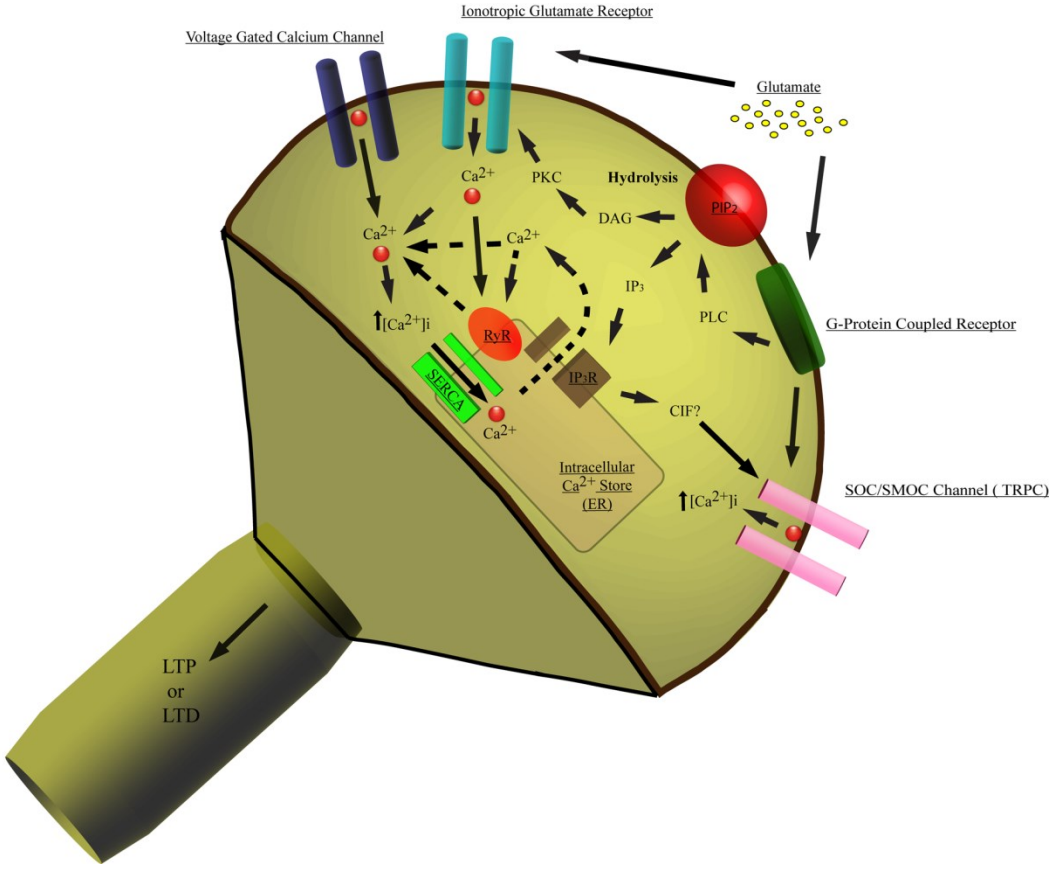

Figure 1.2 - Mechanisms that contribute to elevated intracellular Ca^{2+} *levels at excitatory synapses in neurons - Glutamate can directly activate ionotropic channels, such as NMDA or AMPA receptors, which can lead to* Ca^{2+} *influx. A corresponding change in the membrane potential can activate voltage-gated* Ca^{2+} *channels, leading to further influx of* Ca^{2+}*. Activation of type 1 metabotropic glutamate receptors (mGluRs), which are coupled to G-proteins, produces an intracellular signaling cascade where phospholipase C (PLC) cleaves phosphatidylinositol 4,5 bisphosphate (PIP2) producing diacylglycerol (DAG) and inositol 1,4,5-trisphosphate (*IP_3*). DAG activates protein kinase C (PKC), while IP3 binds to receptors (*IP_3R*) on the endoplasmic reticulum (ER) and releases stored* Ca^{2+}*. Ryanodine receptors (RyR) can also be bound by* Ca^{2+} *and cause* Ca^{2+}*-induced* Ca^{2+} *release. In some types of neurons, release of* Ca^{2+} *from intracellular stores causes additional influx of* Ca^{2+} *through store-operated/second messenger-operated channels (SOCs/SMOCs), which may be mediated by a* Ca^{2+} *influx factor (CIF). SOCs/SMOCs are believed to be transient receptor potential channels (TRPs) in many cells. In Purkinje cells, activation of mGluR1s causes influx of* Ca^{2+} *through TRPCs. Calcium levels are returned to baseline levels by uptake through the sarcoplasmic-endoplasmic reticulum* Ca^{2+}*-ATPase (SERCA) into the ER, by extrusion through membrane pumps, by binding to cytosolic proteins, or by uptake into organelles such as the nucleus and mitochondria.*

A stable cellular mechanism for memory could not be established without an opposing force of plasticity, as synaptic strength can only be depressed so far. LTP provides this opposing force of plasticity by strengthening synapses. In cerebellar PC synapses LTP is observed to occur with PF stimulation alone, this effect is ascribed to increased glutamate release from PF terminals (Salin, Malenka, & Nicoll, 1996). It was recently shown that there is also a postsynaptic LTP effect that occurs with PF simulation that is cAMP independent and relies on nitric oxide (Lev-Ram et al., 2002).

The interplay between LTP and LTD of the PF-PC synapse indicates that it operates bi-directionally (i.e. PF stimulation alone leads to LTP of the synapse, while paired stimulation from PFs and CFs causes LTD.). The bi-directionality is controlled by intracellular Ca^{2+} concentration ($[Ca^{2+}]_i$); where a high $[Ca^{2+}]_i$ favors LTD induction and a low $[Ca^{2+}]_i$ favors LTP induction (Coesmans et al., 2004). This is the opposite result to the effect levels of observed $[Ca^{2+}]_i$ have on plasticity at other known bidirectional synapses in the brain, such as those in the cerebral cortex and hippocampus (Hansel, Artola, & Singer, 1997; Mulkey & Malenka, 1992). Together this indicates that bi-directional plasticity of the PF-PC synapse has a significant functional role as it modulates the excitability of the sole output neuron of the cerebellar cortex, the PC. Changes induced in the cerebellar circuitry surrounding PCs as well its output targets, the deep cerebellar nuclei and vestibular nuclei, signify a change to the internal representation of a stored memory (i.e. various types and degrees of plasticity in different synapses throughout the cerebellar cortex interact to produce and output signal that fine-tunes our motor movements; D'Angelo & DeZeeuw, 2008). This highlights the

significance of proper GC function for overall cerebellar function, as they provide these important PF projections synapsing onto and affecting the firing of PCs

1.3.1 Calcium and Cerebellar Based Ataxia

The cerebellum plays a critical role in learning sensorimotor tasks or skills (Kandel et al., 2000). For instance, it is widely accepted that the olivo-cerebellar tract is a key pathway contributing to motor learning (Ito, 2006). Although the involvement of cerebellar circuit is critical, its precise role in this process is undetermined. There is currently a growing awareness that neurodevelopmental disorders are associated with cerebellar deficits and learning impairments (Manto & Jissendi, 2012). The cerebellum is an excellent platform for studying neurodevelopment as its structural development occurs in a heavily stereotyped pattern and additional development occurs after birth. In addition, the anatomy of the cerebellum has been highly conserved from rodents to humans, suggesting that studies of cerebellar phenomena in rodents should be at least partially applicable to humans (Manto & Jissendi, 2012).

Calcium signaling plays a prominent role in long-term changes in PC synapses with PFs. In Marr-Albus-Ito models of cerebellar function, LTD at PF-PC synapses provides a cellular substrate of certain forms of cerebellar motor learning (Marr, 1969; Albus, 1971; Ito, 1984). Marr proposed that PF synapses onto PCs are potentiated when they are activated simultaneously with a CF (Marr, 1969). In Marr's theory the cerebellum learns motor skills by storing memory traces at the PF synapse under instruction of the olivary nucleus, which signals correct performance via CF activation. A few years later, Albus (1971) refined this theory by suggesting that the cerebellum functions on a modified classical conditioning paradigm, with a complex spike as the

unconditioned stimulus and MF input as the conditioned stimulus. This last hypothesis became known as the Marr-Albus theory, which predicted the existence of LTD before any plasticity of synapses onto PCs was found. The theory was further extended by Ito with his flocculus hypothesis (Ito, 1984). A prominent experimental model of classical motor conditioning is eye-blink conditioning (Medina et al., 2002b). In this model, the conditioned stimulus is a tone, which is paired with the unconditioned stimulus of a puff of air. The resulting conditioned response is the closing of the eyelid when only a tone is presented, and it is this learned response that is believed to be mediated by PF-LTD. PF-LTD can be induced *in vitro* by simultaneous activation of PFs and CFs at low frequencies (Ito & Kano, 1982, Coesmans et al., 2004). In these cerebellar network models, it was assumed that PF-PC synapses carry contextual information and that signaling at CF-PC synapses represents error signals in motor performance that could alter subsequent behavior.

During ataxia, movements are usually characterized by abnormal timing, delayed muscle activation, sudden interruptions, and exaggerated corrections. These dysfunctions, which are fundamentally of timing and coordination, are often due to a lack of cooperation between agonist and antagonist muscle activation (Garwicz, 2002). The deficit in timing likely reflects an abnormal pattern of activity in deep cerebellar or vestibular nuclei, which is thought to encode relative phases of muscle contraction (Sánchez-Campusano, Gruart, & Delgado-García, 2007). Interruptions or alterations in cerebellar circuitry usually leads to some form of ataxia, and more subtle changes that do not interfere with the structure of the circuitry usually do not affect motor performance, only motor learning (DeZeeuw & Yeo, 2005). Mutant mouse models with a disturbed

Ca^{2+} homeostasis all experience ataxia, at least to some degree (Draski et al., 1994; Lalonde & Strazielle, 2001; Mistumura et al., 2011).

Although the PF-PC is arguably the most studied synapse in the cerebellum with respect to plasticity, there are other important synapses with possible functional significance that have recently been described such as the MF-GC synapse (D'Angelo et al., 1999). Plasticity of the MF-GC synapse is bi-directional and has been observed to be NMDA-receptor-dependent. Both LTP and LTD of this synapse are expressed presynaptically via an increase in glutamate release probability as detected by an increased electrophysiological NMDA-receptor-mediated current (Nieus et al., 2006). Unlike the reversal in the PF-PC synapse, a lower $[Ca^{2+}]_i$ will cause the induction of LTD and a higher $[Ca^{2+}]_i$ will lead to LTP induction (Gall et al., 2005). This indicates that the hypothesized abnormal Ca^{2+} levels in *wdl* mice would drastically alter synaptic plasticity and therefore the information processing capabilities of the cerebellum.

In a recent review D'Angelo & De Zeeuw (2008) put forward a 'time-window matching' hypothesis which states that MF inputs to the granule cell layer (GCL) are transformed into "well-timed spike bursts" by intrinsic GCL processing, the duration of which is controlled by GoC feed-forward inhibition. The oscillation of these spike bursts is differentially spread over various fields of GCs so as to generate ongoing time-windows from interacting motor domains (D'Angelo & De Zeeuw, 2008). Synaptic plasticity at this synapse would therefore serve the purpose of fine-tuning certain pre-wired circuits, with the end result of favoring certain granule cell groups with respect to particular time windows. This phenomenon demonstrates that plasticity at GC synapses is

as important for proper cerebellar function as the plasticity at the heavily studied PC synapses.

As many types of cerebellar plasticity at various synapses rely on differential Ca^{2+} concentrations to drive either the strengthening or weakening of that synapse, the importance of proper Ca^{2+} homeostasis becomes clear. Modifications to the abovementioned synapses via altered plasticity would affect the cerebellums' ability to integrate existing motor function with novel incoming information (i.e. vestibular input being integrated with balance motor programs). The effects on plasticity would almost certainly affect motor learning that is known to require cerebellar involvement (Ito, 2006).

1.3.2 Calcium Dependant Long-Term Plasticity in the Cerebellum

Purkinje Cells

The PC is one of the brains largest neurons, second only too large cortical pyramidal neurons, with a large dendritic arbor. PCs receive two types of excitatory input that, depending on timing and the source of input, can cause two distinct electrophysiological phenomena; either a simple spike, which can also occur spontaneously, or a complex spike that is slower and begins with a large amplitude response followed by a small amplitude burst (Kandel et al., 2000). One major excitatory input to PCs is the PFs which arise from a multitude of GC axons running from the GCL into the ML where they are oriented parallel to the long axis of the cerebellar folia. The second excitatory input comes from the CF which originates in the inferior olivary complex and transmits both sensory and motor information from the brain stem (Dean et

al., 2010). Each PC contacts and synapses with only one CF in adulthood as opposed to the PFs which can synapse up to 100,000 times with distal PC dendrites (Ito, 2006).

Activation of groups of PFs *in vitro* causes the release of glutamate into the synaptic cleft, which results in brief excitatory postsynaptic potentials (EPSPs; Eilers et al., 1995) in PCs. If the stimulation intensity is high enough, the result is the generation of action potentials in PCs termed simple spikes, which can occur at various frequencies *in vivo* depending on various vestibular and motor signals (Barmack & Yakhnitsa, 2003; Dean et al., 2010). Activation, and release of glutamate from CFs, causes an all-or-none response leading to a strong EPSPs in PCs termed a complex spike, which is a unique action potential observed in PCs (Dean et al., 2010). The complex spike is a multi-component waveform believed to consist of an initial somatic sodium spike followed by several smaller Ca^{2+} spikes generated in dendrites (Schmolesky et al., 2002; Weber et al., 2003). Both PF and CF-mediated electrical responses in PCs are produced through α-amino-3-hydroxy-5-methyl-4-isoxazolepropionate (AMPA) receptor activation (Eilers et al., 1995; Schmolesky et al., 2002), which subsequently leads to an influx of Ca^{2+} through VGCCs. The most numerous type of VGCCs in PCs are of the P/Q type, however some influx is through L-type channels, with very little contribution from N-type VGCCs (Empson & Knopfel, 2010). Recently, currents mediated by *N*-methyl-D-asparate (NMDA) receptors have been measured at CF-PC synapses (Piochon et al., 2007; Renzi et al., 2007; Piochon et al., 2010), therefore influx through these receptors also contributes to Ca^{2+} signaling in PCs.

The repetitive stimulation of PFs *in vitro* appears to activate two signaling pathways in PCs. The first is a rapid influx of Ca^{2+} through VGCCs caused by the

depolarization of the membrane by AMPA receptor activation described above; and the second involves a delayed release of Ca^{2+} from intracellular stores caused by the production of IP_3 by metabotropic glutamate receptors (mGluRs; Finch & Augustine, 1998). CNQX, an AMPA receptor antagonist blocks the initial but not the late rise in Ca^{2+}. Others have also demonstrated that glutamate causes a large and transient increase in dendritic Ca^{2+} in both Ca^{2+}-containing and Ca^{2+}-free media, indicating that part of the increase in Ca^{2+} is attributable to release from intracellular stores (Llano et al., 1991).

Experiments have shown that mGluR antagonists have little effect on glutamate induced production of IP_3 in cultured PCs, but that the AMPA receptor antagonist CNQX can block most of the glutamate-mediated IP_3 production (Okubo et al., 2001). In this preparation, AMPA receptor activation, and the resultant depolarization and activation of VGCCs, is specifically required for IP_3 production. These results were repeated in acute cerebellar slices, in which electrical stimulation of CFs induced IP_3 production. However, only PF and CF co-activation produced sufficient IP_3 levels to activate IP_3 receptors, leading to an increase in Ca^{2+} in the spines of PCs (Okubo et al., 2001). In another study conducted *in vitro*, the depletion of ER Ca^{2+} stores instigated the docking of the ER to the plasma membrane, where IP_3 receptors could open store-operated Ca^{2+} channels (Ma et al., 2000), similar to a capacitive mechanism reported in other neuronal types (Weber et al., 2001; Baba et al., 2003). Under some experimental conditions, activation of PFs or CFs produces an mGluR-mediated slow membrane conductance (Tempia et al., 2001; Dzubay & Otis, 2002; Yuan et al., 2007). It has also been demonstrated that mGluR1 activation is physically coupled to activation of TRPC1 membrane cation channels at PF synapses, which allow additional influx of Ca^{2+} into PCs (Kim et al., 2003). This TRPC1

channel appears to be responsible for the mGluR mediated slow membrane potential conductance at PF-PC synapses. Therefore, glutamate receptor activation appears to stimulate a wide variety of mechanisms, which can lead to Ca^{2+} elevation in PCs.

The efferent signals of PCs provide GABAergic inhibition to its target neurons in the vestibular and deep cerebellar nuclei (Ito, 2006). PCs provide 73% of the total afferent synaptic contacts to the two nuclei mentioned above, which includes almost all incoming somatic information (De Zeeuw & Berrebi, 1995). In acute rat slices, tetanic stimulation of inhibitory synapses on deep cerebellar nuclei neurons, presumably derived from descending PC axons, resulted in long term depression (LTD) of these synapses. The LTD is the result of postsynaptic GABA desensitization caused by an increase in $[Ca^{2+}]_i$ activating protein phosphatases (Morishita & Sastry, 1996). Deep cerebellar nuclei neurons also display a pronounced rebound depolarization in the form of a large sodium spike following an injected hyperpolarizing current, which was thought to mimic PC input (Aizenman & Linden, 1999). These two types of plasticity observed in cerebellar nuclei neurons are hypothesised to be a site for long term cerebellar-mediated motor memory storage (Ito, 2006).

Granule Cells & Mossy Fiber Projections

GCs are the most numerous neuronal type in the brain, and in the cerebellum are arranged stereotypically in the GCL. Understanding how the GCL processes incoming information is important; as the sole output from this layer, the PFs, provides one of the main inputs to PCs. There is strong evidence that PF synapses on the ascending axonal segment of GCs have a substantial influence on motor output by manipulating the timing of PC firing (Lu, Hartmann, & Bower, 2005). This hypothesis is in agreement with a

review published which reaffirms that GCs have an important computational role in the cerebellum and indirectly affect the motor output of an organism by altering temporal patterns of PC activation (D'Angelo & De Zeeuw, 2008). Plasticity at the MF-GC synapses is proposed to be the mechanism for dictating the timing of PC output. The diffuse information processing capabilities of the GCL spread over populations of GCs and the large effect the GCL exerts on PC firing make the numerous GCs of the cerebellum an interesting experimental subject, especially as little research has been previously conducted on this neuronal population.

As mentioned above, MFs are one of the major inputs to the cerebellum that arises from precerebellar nuclei such as the spinal cord, reticular formation, and both pontine and vestibular nuclei (Eccles et al., 1967; Ito, 2006). A MF glomerulus is formed when MF glutamatergic projections synapse with up to 100 GCs along with inhibitory Golgi cells (GoCs; Ito, 2006). At the center of the glomerulus is a MF rosette, which is simply a series of enlargements along the MF axon that many neighboring GCs synapse onto. The MF rosettes may be "simple" or "complex" depending on if they are spherical or have a more intricate "knotted" structure, respectively. A glial sheath encloses the entire glomerulus and insures signaling is kept chemically separate from extra-synaptic fluid (Jakab & Hamori, 1988). Excitatory post-synaptic currents (EPSCs) in GCs that are generated through MFs are very important to cerebellar function, as they are the major excitatory input to the cerebellum. Equally as important to proper signaling, GABAergic inhibitory post-synaptic currents (IPSCs) from the GoCs can modulate the probability of an EPSC being generated at the MF-GC synapse (Ito, 2006).

Recordings from cerebellar slices have demonstrated that Ca^{2+} currents in MFs are inhibited by stimulating GoCs for at least 1s at high frequency, i.e. 50 Hz (Mitchell & Silver, 2000), which is a frequency of stimulation observed *in vivo* during limb movements (van Kan et al., 1993). Subsequent *in vitro* studies showed that this inhibition occurs primarily via GoC-mediated $GABA_B$ receptor activation that has been shown to be a persistent process (Thomsen et al., 2010). By affecting Ca^{2+} signaling in MFs, GoCs may be modulating the long-term strength of the MF-GC synapse via long term potentiation (LTP) or LTD of the synapse (Gall et al., 2005). Normally GoCs interact with the MF-GC synapse indirectly such as via neurotransmitter spillover (i.e. neurotransmitter released at one synapse diffuses and stimulates neighboring synaptic connections), but occasionally the GoC will have a direct synapse to the glomerulus (Mitchell & Silver, 2000).

Since a MF complex rosette is a relatively large structure, it is thought that localized signal processing may occur within it (Ito, 2006). The possibility of compartmentalized signaling indicates that hypothetically both LTP and LTD of the MF-GC synapse can occur in glomeruli located closely together. This is due to GoC IPSC modulating surrounding GCs to different degrees depending on how many GoC-GC synaptic connections exist (Thomsen et al., 2010). Since the glomeruli are how GCs receive their primary afferent connections, variable plasticity in closely localized glomeruli would help to ensure afferent information to the cerebellum from one area is not contaminated by that from another. This afferent information to the cerebellum is important for its proper function, as vestibular and somatosensory feedbacks are vital for proper motor learning and performance (Ito, 2006).

MFs have an important role in motor learning in the cerebellum because of the synapse they make with GCs (Nieus et al., 2006). Calcium plays a vital role in LTD and LTP of the MF synapse; it is required for many underlying cellular mechanisms of plasticity. Plasticity involving MF-GC synapses is essential as the first stage of information processing in the cerebellar circuitry. This plasticity drives LTD and/or LTP of the ML interneurons which need to work in concert with the PFs in order to properly excite/inhibit affecting spike timing in PCs. An ataxic model, the *tottering* mouse, was observed to display timing irregularities of PC firing (Hoebeek et al., 2005) indicating that abnormality in timing of PC output can significantly affect motor output. Interestingly, the ability for motor learning was affected yet there was no general ataxia seen in animals. It was previously demonstrated that if ML interneurons have neurotransmission blocked, then ascending signals from the GCL are unable to properly coordinate ML plasticity, and proper consolidation of motor learning was significantly reduced (Schonewille et al., 2007). Since the cerebellum is essentially driven by its input, irregularities in the GC populations which first processes that input would have adverse effects as the incoming information travels further through the cerebellum. Taken together these studies on GCs and their input, the MFs, show a vital role for the GCL in proper motor output; especially when this output involves motor learning of some kind.

Golgi Cells

The GoC is the major inhibitory interneuron of the cerebellar GCL (Ito, 2006). A cerebellar neural network simulation model estimates that each GoC is innervated by ~4790 excitatory inputs from PFs in the ML and ~290 MF terminals in the GC layer (Pellionisz & Szentagothai, 1973). Histological analysis demonstrates that the GoC

extends a considerably branched axon that innervates ~5700 GCs, providing them with inhibitory GABAergic input (Palkovits et al., 1971). In most cases, synaptic plasticity is reliant on an intracellular increase of Ca^{2+} that activates downstream molecular mechanisms. However, LTD of the PF-GoC synapse has recently been shown to be a process independent of Ca^{2+} and NMDARs (Robberechts et al., 2010). This makes the PF-GoC synapse one of the few that expresses plasticity independent of intracellular Ca^{2+} levels.

Recent experiments have shown that the PF-GoC synapse can undergo LTD with an induction protocol that is similar to physiological signaling from sensory stimulation (Chadderton et al., 2004; Zhang & Linden, 2006; Robberechts et al., 2010). This physiological input pattern required for PF-GoC LTD is quite similar to the induction protocol for PF-PC LTD (Coesmans et al., 2004; Sims & Hartell, 2006). GoCs have LTD induced by consecutive stimulation of peripheral afferents and CFs, but not by stimulation of peripheral afferents alone (Xu & Edgley, 2008). GoCs plasticity being dependent on afferent CF activation contributes to theories of cerebellar-mediated motor learning, since many of them propose the dependence of cerebellar motor learning on the timing of inputs (Ito, 2006; D'Angelo & De Zeeuw, 2008).

PF-GoC LTD is strongly dependent on the AMPAR subunit $GluR_2$, which is also a biological marker for GoCs. Although GoCs can display plasticity of their PF synapses independent of NMDAR activation (Robberechts et al., 2010), activation of AMPARs containing the $GluR_2$ subunit generally result in strong NMDAR activation (Kullmann & Lamsa, 2007). Both hippocampal and cortical synapses which post-synaptically express

the $GluR_2$ subunit and experience LTD can also experience plasticity independent of NMDAR activation (Otani et al., 2002; Poschel & Manahan-Vaughan, 2005).

There have been several studies conducted that connect GoC LTD to cerebellar motor learning (Dugué et al., 2009; Xu & Edgley, 2008). GoCs have a vital role in cerebellar signaling by regulating the silencing and timing of GCs (Tahon et al., 2005), which is believed to create an oscillatory behavior within the GCL (D'Angelo 2008). A recent study has shown that GoCs are connected via extensive gap junctions which allow them to display this low-oscillatory timing of inhibition of GCs (Dugé et al., 2009). GoC plasticity therefore affects the timing of the major excitatory input circuit of the cerebellum (Ito, 2006; Dugé et al., 2009).

GoCs are currently hypothesized to play a larger role than traditionally thought in cerebellar motor learning by significantly modulating the excitability of cerebellar neurons. The recently elucidated oscillatory behavior of the GoC-mediated inhibition over fields of GCs could be a vital component of motor learning and one of the few examples of Ca^{2+} independent plasticity in the cerebellum.

Inhibitory Interneurons

Research on smaller inhibitory interneurons has fallen behind that of larger cells, principally because traditional methods are biased towards recordings from neurons with large somas (Jörntell et al., 2010). These interneurons have an important modulatory role and synapse with PFs as well as PCs (Ito, 2006). Inhibitory interneurons have many roles that can range from global network inhibition affecting broad signaling in the cerebellar circuitry to direct electrical coupling allowing neighboring interneurons to fire in synchrony (Mann-Metzer & Yarom, 1999). Cerebellar interneurons are generally divided

into basket and stellate cells and although there are morphological differences, recent studies have indicated that they have similar functionality (Jörntell & Ekerot 2003). The main excitatory input to the interneurons comes from PFs and the major inhibitory input is neighboring interneurons and occasionally GoCs (Eccles, 1967). Interneurons also receive stimulation from CFs, and evidence suggests that a possible mechanism for this observation is that glutamate released from CFs acts at other synapses, such as PF synapses distributed throughout these cells (Jörntell & Ekerot, 2003; Szapiro & Barbour, 2007).

Cerebellar interneurons fire spontaneously at rest and it is because of this that there tends to be a strong EPSP-to-spike coupling at the PF-interneuron synapse (Carter, 2002). This means that single synaptic inputs can exert powerful effects on the interneurons of the cerebellum; interestingly, interneurons of other brain regions, e.g. the neocortex, are modulated by a larger number of weak synapses (Bruno et al., 2006). A recent *in vitro* study indicated that the PF-interneuron synapses with the largest responses may express Ca^{2+}-permeable AMPARs (Liu & Cull-Candy, 2000). If the larger activations are mediated by Ca^{2+}-permeable AMPARs then this could mean Ca^{2+} imaging techniques could image activity at the PF synapse level of the cerebellum (Jörntell et al., 2010; Wilt et al., 2009).

Additional *in vitro* studies have indicated that repetitive PF activation could reduce the Ca^{2+}-permeability of AMPARs on interneuron synapses (Liu & Cull-Candy, 2002; 2005). The Ca^{2+}-permeable AMPARs were replaced with non- Ca^{2+}-permeable AMPARs in the previous protocol, causing there to be a net LTD. Since plastic processes are generally bidirectional, then the insertion of Ca^{2+}-permeable AMPARs should have

the opposite effect of inducing LTP. Studies did show it is possible to do this and achieve large EPSPs (Jörntell & Ekerot, 2003). LTP of the PF-interneuron synapses *in vitro* requires both NMDA activation and Ca^{2+} influx, whereas LTD only requires Ca^{2+} influx through Ca^{2+}-permeable AMPARs (Rancillac & Crepel, 2004). NMDAR activation in the interneurons is dependent on CF excitatory input as well as PF stimulation (Barbour et al., 2007); this coincides with *in vivo* findings that CF and PF concurrent stimulation is necessary for LTP induction, but PF activation alone can induce LTD (Jörntell et al., 2010).

The inhibitory interneurons also exhibit plastic synapses with PCs. The plasticity expressed here is associative because it requires simultaneous activation of an interneuron-PC synapse and depolarization of the PC (generally via CF input) (Kano, 1996). This plasticity is expressed as a potentiation of IPSCs from interneurons to PCs (Mittmann & Häusser, 2007). Some reports of paired CF and interneuron activation indicated a potentiation (Kano, 1996), but there were other groups reporting a depression in IPSCs (Mittmann & Häusser, 2007). This discrepancy may be a result of differences in Ca^{2+} levels obtained after CF stimulation. Since the inhibitory interneurons providing inhibition to the PCs can be spiked with the same PF input, plasticity of this synapse will not change the source of inhibition in the PC (Jörntell et al, 2010).

In the classical conditioning eye blink reflex paradigm, there is a timed silencing of PC activity; presumably to release deep cerebellar nuclei from PC inhibition to allow for the eye blink to take place (Hesslow, 1994). The eye blink reflex is also coupled temporally to PC silencing (Svensson et al., 2010). This temporary attenuating of PC activity seems to rely on inhibitory interneurons to silence PCs. Investigations of this

phenomenon suggest that the inhibitory interneurons contribute to the underlying mechanisms of the conditioned eye blink response, showing that there is increased spontaneous GABAergic activity into the PC up to 24 hours after training (Scelfo et al., 2008). Therefore, the GABAergic interneurons may have an important role in motor learning by PC inhibition.

Interneurons are suggested to function by either global inhibition or local feed forward inhibition. The GoCs seem to operate through global inhibition, utilizing their extensive dendritic arbor (Dieudonné, 1998). The cerebellar interneurons fit more in the second category as they are configured to modulate cerebellar output with high spatial and temporal specificity (Jörntell et al., 2010). This is why these interneurons are likely involved in cerebellar mediated motor learning.

The cerebellum has long been accepted as a part of the brain involved with fine motor coordination and learning. As described, there are many components to the circuit in the cerebellar cortex. Original motor learning theories suggested that learning took place solely at the synapses between PFs and PCs, and that most; if not all other synapses in the cerebellar cortex were not plastic. Clearly, this view was overly simplistic, as plasticity has now been described at several synapses in the cerebellar cortex. Therefore, even if memories are stored at PF-PC synapses, alterations or plasticity at synapses upstream of PF-PC synapses could affect the ability to have PF-LTD induced. For example, LTD at GC synapses with MFs may lead to less firing of PFs, which could decrease the ability of PF-LTD to be induced.

1.4 Mutant Ataxic Animal Models

Immense strides have been made in advancing techniques used to research the involvement of Ca^{2+} in cerebellar plasticity and motor learning. One of these novel techniques is the use of genetic knock-out, knock-in, or mutant mice which allows for this phenomenon to be studied *in vivo*. At the center of most types of synaptic plasticity in the cerebellum is the Ca^{2+} ion. Calcium appears to be necessary for the induction of LTD and LTP at most synapses, and a wide variety of animal models (mutant or transgenic) that elicit disruptions in motor function, have alterations in various components of Ca^{2+} signaling pathways.

Many varieties of ataxic mutant mice are suitable for studies of cerebellar plasticity and signaling; such as the hotfoot mouse (Draski et al., 1994; Mandolesi et al., 2009). The hotfoot mouse has a single recessive gene (*ho*) causing a resting body tremor and a high quick-stepping pattern during movement due to alterations in monoaminergic neurotransmission (Draski et al., 1994). There are also more recently discovered models with altered plasticity in the cerebellum, such as the voltage gated $K_{V3.3}$ channel knockout mouse that experiences irregular Ca^{2+} dynamics and electrical conductance in PCs (Zagha et al., 2010).

Recently, Schonewille, et al., (2010) reported that LTD may not be the only process responsible for motor learning in the cerebellum. This study employed a PC-specific knockout of Ca^{2+}/calmodulin-activated protein-phosphatase-2B (PP2B) based on previous research indicating that PP2B interacted with α-CaMKII to change the phosphorylation state of AMPA receptors (Lisman & Zhabotinsky, 2001). By disrupting

PP2B production in PCs LTP was abolished and motor learning was impaired, while LTD remained unaffected (Schonewille, et al., 2010). Previously, much of the focus of cerebellar learning researchers was exclusively on LTD. However, Schonewille, et al., (2010) indicated that LTP is also an important facet of motor learning and may complement other types of plasticity by controlling excitability. Since in the Schonewille experiments above LTD alone was found insufficient for proper vestibule-ocular reflex (VOR) conditioning, but the kinetics of VOR were unaffected; a 'priming' effect for LTP is plausible.

Other transgenic animals available for ataxic research involving plasticity within the cerebellum include an mGluR null mutant (Alba et al., 1994) and the *stagger* mouse (Mistumura et al., 2011). The *stagger* mutation results in a functional loss of a transcription factor, Retinoid-related Orphan Receptor α (RORα), which is typically prevalent in cerebellar PCs. The most prominent result of the lack of RORα at PC synapses is the complete loss of mGluR-mediated EPSCs. With this in mind, it can be seen how the novel *stagger* mutation and the mGluR-null mutation can provide complementary data. Animals bred from the aforementioned models exhibit similar ataxic behaviour, and an impairment of LTD (Alba et al., 1994; Mistumura et al., 2011). The key difference is that the mGluR-null model is completely devoid of any mGluR protein; whereas, the *stagger* model is missing the mGluR-mediated retrograde suppression of PF EPSCs via endocannabinoids and mGluR-mediated slow EPSCs in PCs. Therefore, the functions of the mGluR that are impaired in *stagger* mice may be responsible for the similar ataxia and LTD impairment in mGluR-null mice. Although VGCCs were shown to not be affected by Alba et al., (1994); Ca^{2+} release has been

shown to be important for LTD and there may be a dysfunction of IP_3-mediated intracellular Ca^{2+} store release in these two models. The reason for this is that the mGluRs found in PCs have been shown to activate the IP_3-mediated intracellular Ca^{2+} store release (Okubo et al., 2001), leading to LTD.

Some transgenic models have allowed us to discover and study novel phenomena, *in vivo*. Cellular prion protein (PrP^C) is an excellent example of this, since despite years of research there is little known about its physiologic role or the role played in several neurodegenerative diseases. A recent study utilized PrP-knockout mice to investigate the involvement of PrP^C in Ca^{2+} dynamics (Lazzari et al., 2011). In the PrP-knockouts, there was a dramatic increase of store operated Ca^{2+} entry which was found to be due to a lower expression of Ca^{2+}-ATPases in the plasma membrane as well as ER. The loss of regulation of extracellular Ca^{2+} influx led to an increased susceptibility to excitotoxicity and therefore to cell death (Lazzari et al., 2011). This is a likely mechanism by which bovine spongiform encephalopathy and other related prion diseases progress so rapidly and aggressively. Although these mice experience disruption of cerebellar Ca^{2+} homeostasis, there seems to be only a small effect on learning and memory in the cerebellum (Steele, et al., 2007). This is likely due to LTD being intact, and only the pace making ability of PCs seems to be affected.

Since the mechanisms underlying plasticity of the cerebellum are numerous, generally sensitive to modulation, and are best studied *in vivo*; cerebellar plasticity research lends itself to the use of transgenic models. The continued use of these models and other approaches will aid in evolving this field of research towards a greater and more in depth understanding of how cerebellar circuits works to store motor memories.

1.5 The Waddles Mouse and CAR8

The spontaneous mutation which yields the *wdl* mouse is due to non-functional expression a particular protein, CAR8 (Jiao et al., 2005). The absence of CAR8 appears to cause ataxia with a side-to-side 'waddling' gait as it is the only protein altered by the *wdl* mutation; even though functional CAR8 lacks any known enzymatic activity (Dodgson et al., 1991). However, CAR8 has been shown to have a high affinity for the IP_3R which gates intracellular ER Ca^{2+} stores (Hirota et al., 2003). It therefore seems plausible that the *wdl* mice are experiencing ataxia due to Ca^{2+} dynamics-related interference with plasticity. Supporting this hypothesis, a study conducted with IP_3R1 null mice found that both cellular signaling and LTD were affected by the lack of this receptor (Nagase et al., 2003). CAR8 and the dysfunction caused by its absence are the major focuses of this research project.

The family of carbonic anhydrases are metal-containing enzymes which are fundamental to many biological phenomena such as: photosynthesis, respiration, and bone reabsorption (Dodgson et al., 1991). CAR8 is one of three acatalytic proteins within the sixteen members of the family. The lack of enzymatic activity observed is due to missing one or more Zinc binding histidine residues. The CAR8 protein is expressed most abundantly in the cerebellum in the CNS with particularly high levels in PCs and ML, indicating a strong possibility for a role in brain functions (Aspatwar, Tolvanen, & Parkkila, 2010). There was weak, but significant, expression of CAR8 seen in the GCL (Aspatwar, et al., 2010). Immunohistochemistry showed CAR8 protein in neural cell bodies as well as neurites in the adult mouse cerebellum (Taniuchi et al., 2002). Although

there is detectable expression throughout bodily tissues, CAR8 is expressed at only one fifth the level seen in cerebellar tissue in the lungs and liver; which are the only two other tissues expressing significant levels (Aspatwar, et al., 2010). A recent developmental expression study of CAR8 indicated it is widely distributed throughout all developing tissue at early stages (0 – 11.5 days post-impregnation) of development (Lakkis, O'Shea, & Tashian, 1997). The level of expression appeared to be regulated temporarily in a tissue-specific fashion and as development progressed, the expression become more restricted (similarly to the adult expression profile).

IP_3 and its receptor are integral components of the Ca^{2+} system keeping intracellular Ca^{2+} dynamics balanced (Fig. 1.2). This signaling pathway is clearly important for normal Ca^{2+} signaling since it is connected with group I mGluRs which would be activated often by glutamatergic transmission. CAR8 normally inhibits the binding of IP_3 released from group I mGluR activation to the IP_3R and therefore regulates the amount of Ca^{2+} released from intracellular stores. There is evidence that CAR8 is also an important protein for proper development of the cerebellar cortex and the arrangement of excitatory synapses (Aspatwar et al., 2010). A previous study of *wdl* mice found abnormal extension of CFs into the ML of the cerebellar cortex in *wdl* mutants, a significant number of PC spines not forming synapses with PFs, and multiple synapse varicosities at many PF-PC synapses (Hirasawa et al., 2007). These structural abnormalities are likely caused by the decreased responsiveness of IP_3-mediated ER Ca^{2+} stores in the *wdl* mutant. The ataxia could also be related to the lower number of functional synapses formed in the cerebellar cortex of homozygous animals. This would once again indicate that altered Ca^{2+} levels are not only affecting proper signaling, but

proper development of the cortex and synapses within it. The ataxia experienced by *wdl* mice could be due directly to the suspected atypical Ca^{2+} signaling, but more likely to the abnormal development linked to the atypical Ca^{2+} signaling at both pre- and post-natal time points.

Other ataxic mice, such as the *tottering* and *leaner* mutants, have similar issues to the *wdl* with respect to the aberrant cerebellar morphology and altered Ca^{2+} levels (Lalonde & Strazielle, 2001). *Cacna1a* encodes for the α-1a subunit of P/Q type VGCCs; the knockout of which causes the ataxic syndrome seen in *tottering* mice. *Tottering* mice exhibit a disruption in PC firing and display motor deficits, which are similar to ataxic syndromes in patients (Hoebeek et al., 2005). Similar to the *wdl* mutants, *tottering* mutants also display multiple synaptic varicosities and abnormal expansion of PF territories (Miyazaki et al., 2004). In both the *tottering* and the *wdl* mice there is a similar underlying issue of abnormal intracellular Ca^{2+} signaling (Kurihara et al., 1997). This provides evidence that the development of cerebellar cortex is sensitive to changes in Ca^{2+} concentrations and that this can significantly affect motor output. *Leaner* mice also exhibit disrupted motor function, similar to CACNA1A knockout mice (Rhyu et al., 1999). This P/Q-type channel subunit is highly expressed in cerebellar PCs in approximately 90% of VGCCs; and also in GCs in approximately 45% of VGCCs (Randall & Tsien, 1995).

All of the mutations mentioned above are linked as they featured significant disturbances in cerebellar Ca^{2+} signaling as an underlying pathophysiology and also multiple synaptic varicosities being formed at PF-PC synapses (Rhyu et al., 1999). Multiple synaptic varicosities is a similar morphological phenotype to that seen in the *wdl*

mice which progresses over the first three weeks post-natally. The similarities between the *wdl* phenotypic morphological abnormalities and those displayed by many other ataxic mutants with altered Ca^{2+} signaling indicate an important developmental role for Ca^{2+} in the juvenile murine cerebellum. Disturbing the natural homeostasis of Ca^{2+} in the cerebellum seems to inevitably lead to some form of ataxia.

The *wdl* mouse was utilized for this study since relatively little is known regarding the pathology of the observed ataxia, aside from the involvement of CAR8 (Jiao et al., 2005) and morphological abnormalities which are possibly the cause of decreased functional excitatory signaling (Hirasawa et al., 2007). The localization of the ataxia inducing mutation to mainly the cerebellum in *wdl* mice, allows for studies to be conducted with less confounding variables that would occur in the other ataxic animal models whose alterations in calcium signaling affect a wide array of brain regions. Calcium imaging studies have not been conducted in *wdl* mice before and their completion allows for hypothesized suggestions of the involvement of CAR8 with intracellular calcium signaling in the *wdl* mutant to be confirmed. These studies will also provide insight into the common pathological underpinnings of cerebellar based ataxias.

1.6 Study Objectives

The aims of this study are to:

- Further characterize the ataxia experienced by both homozygous and heterozygous *wdl* mice.

- Investigate whether Ca^{2+} signaling in the GCL of an acute cerebellar slice preparation is significantly altered in *wdl* mice.
- To characterize any observed differences and link these findings to the known *wdl* pathophysiology.

At the center of most types of cerebellar synaptic plasticity is the Ca^{2+} ion. Calcium appears to be necessary for the induction of LTD and LTP at most synapses, and a wide variety of animal models (mutant or transgenic) that elicit disruptions in motor function, have alterations in various components of a given Ca^{2+} signaling pathway. Although PCs have received the most research attention in the cerebellum, the GCL is also an important computational component of the cerebellum that processes a multitude of incoming information and also provides one of the two main excitatory inputs to PCs. Plasticity in the GCL is highly dependent on $[Ca^{2+}]_i$ and could therefore theoretically be disturbed by altered Ca^{2+} signaling. By altering plasticity in the cerebellum you affect a given organisms ability to fine tune muscle movements and to display effective motor learning. The completion of this research will produce important information regarding the mechanisms of CAR8 function in the cerebellum, and will aid, specifically, in determining the altered cellular physiology of granule cells that may underlie ataxia in the wdl mouse. Since the normal function of CAR8 is to inhibit IP_3 binding and ataxic mutants lack this protein, I hypothesize that normal intracellular Ca^{2+} signaling in granule cells is altered, and that these alterations are underlying the phenotypic ataxia.

Chapter 2 Materials and Methods

2.1 Materials

The following is a list of utilized chemicals and their manufacturers. (S)-3,5 dihydroxyphenylglycine (DHPG) and 1-aminoindan-1,5-dicarboxylic acid (AIDA) were obtained from Tocris BioScience (Bristol, England). L-Glutamic acid and all chemicals used in mixing artificial cerebrospinal fluid (aCSF) were obtained from Sigma-Aldrich, Ontario: Canada. The calcium indicator, Oregon Green 488 BAPTA1-AM (OG-BAPTA-1-AM), was obtained from Invitrogen (Burlington, Canada).

2.2 Animals

All experiments and mouse husbandry were conducted in accordance with the Canadian Council on Animal Care guidelines and with approval from the Institutional Animal Care Committee of Memorial University of Newfoundland. A colony of waddles (*wdl)* mice was started and maintained in the Animal Care Facility at Memorial University of Newfoundland with a breeding pair, originally obtained from Jackson Labs (Bar Harbour, United States), consisting of a homozygous (*wdl/wdl)* female and heterozygous (+/*wdl*) male. Subjects were divided into three groups based on their genotype (WT, heterozygous *wdl*, and homozygous *wdl*). Both mutant animal and WT controls are from the same genetic background (C57 Black); thereby reducing the possibility of genetic differences, aside from the mutation of interest, affecting obtained results. Heterozygotes are generally utilized as controls since they express only one faulty copy of the gene and therefore do not display the phenotypic ataxia. Despite this a WT

group was also included for comparison purposes as the heterozygous mutation may still have a detectable effect on motor output. All mice had food and water available *ad libitum* and were on a 12- hour day/night cycle. Genotyping was unnecessary as the initial breeding pair was genotyped before purchase, and their offspring would have to be either a homozygous or heterozygous mutant. Differentiating heterozygous mice from homozygous mice is relatively simple as only the homozygous animals' display motor difficulties from birth (Harris et al., 2003).

2.3 Rota-Rod

Behavioural experiments were conducted to test motor learning skills utilizing a rota-rod apparatus with a previously established accelerating rota-rod (ARR) paradigm (Jones & Roberts, 1968). An ARR paradigm was chosen as it has been shown to better characterize differences between mutant ataxic mouse strains and test for evidence of motor learning; as opposed to the alternative fixed speed rota-rod paradigm which better characterizes motor impairments due to drug exposure (Rustay et al., 2003). Motor learning in mutant groups was defined as a significant increase in mean rota-rod performance (i.e. a higher latency to fall) on the last day of trials (Day 5) as compared to the first day (Zlomuzica et al., 2012). This increase had to be proportional to that experienced by the WT group which would be expected to display normal motor learning. Subjects must display good balance, coordination, and motor planning to remain on the rotating cylinder. Testing groups were divided by both genotype (*wdl/wdl, +/wdl, +/+*) and age (>six months, six months, three months, one month). The greater than six months

PNA (post natal age) group had an age range of six to nine months. Groups were composed of both sexes.

All ARR trials were conducted during the late morning (i.e. 10:00 – 11:00). Mice were acclimated to the rota-rod obtained from Harvard Apparatus (Barcelona, Spain), turning at four rotations per minute (r.p.m.) for five minutes prior to data acquisition on the first day of testing. The testing schedule consisted of five trials that were 300 seconds in length on day one; followed by two trials on days two through five, also 300 seconds in length. Animals were returned to their home cage for 45 minutes between every trial. At the beginning of each trial the rota-rod began at a speed of four r.p.m. and gradually increased to a maximum speed of 40 r.p.m. over the 300 second trial. The time it took each mouse to fall, or their 'latency to fall', was recorded, digitized, and sent to a connected computer for later analysis; therefore removing some possible human error that would be introduced by manual data collection.

2.4 Slice Preparation

Acute sagittal slices (200-μm thick) were prepared from the cerebellar vermes of one to two month old (range: 21–45 post-natal days) WT, homozygous, and heterozygous *wdl* mice. Imaging experiments were conducted on a different cohort of animals than those utilized for the ARR experiments. Experimental n are reported in this thesis as number of animals. There were generally four slices per animal obtained and three randomly chosen well-loaded cells in each slice analyzed. Data obtained were averaged 'per slice' for final analysis. In all cases, slices were harvested from the subjects'

cerebellar vermes. Subjects were completely anesthetized via inhalation of Halothane before being sacrificed by decapitation. The entire brain was then dissected out and the cerebellum placed in ice cold (0-2 ºC) standard aCSF (in mM; 124 NaCl, 5 KCl, 1.25 Na_2HPO_4, 2 $MgSO_4$, 2 $CaCl_2$, 26 $NaHCO_3$, and 10 D-Glucose) bubbled continuously with 95% O_2 and 5% CO_2. The cerebellar vermis was dissected and then sliced using a Vibratome (Leica). Slices were transferred from the slicer to a large aCSF bath (500 ml) on small pieces of filter paper and suspended on a mesh screen while the solution was bubbled with 95% O_2 / 5% CO_2 for a short period of post-slicing rest (15 minutes). The slices were then transferred to a smaller bubbled bath (20 ml; 22-24 ºC) and bulk loaded with OG-BAPTA-1-AM for one hour (50µg; mixed with 8 µl DMSO, 2 µl pluronic acid, and 90 µl aCSF; yielding a final concentration of 200 µM in the bath; Chuquet, Hollender, & Nimchinsky, 2007; Dawitz et al., 2011). Before imaging, the slices were transferred a final time to a bubbled container with 20 ml of indicator-free aCSF and allowed to rest for 30 minutes.

2.5 Fluorescence Imaging

Fluorescence excitation was provided by the X-Cite Series 120 illumination source (Mississauga, Canada) at 488 nm and visualized at 507 nm. The fluorescence was imaged using a Sensicam 12-bit cooled CCD camera (Kelheim, Germany) and recordings were performed on a Carl Zeiss Axio Examiner D1 (Oberkochen, Germany). During the test period for agonist wash-in recordings an image was taken, with an exposure time of 80 milliseconds, every five seconds over a total time of seven minutes. During electrical

stimulation alone, an image was taken every 3 seconds for a total time of six minutes with an exposure time of 80 milliseconds. When electrical stimulation was combined with AIDA application, an image was taken every 3 seconds for a total of seven minutes, with an exposure time of 80 milliseconds. Data acquisition and analysis were conducted using the Scanalystics IP Lab software (Billerica, United States).

Areas from the GCL were chosen for recording randomly, however areas with no well-loaded cells were avoided. A large area of the GCL would be recorded and later regions of interest (ROIs) around well-defined neuronal somas were chosen for analysis. The number of somas analyzed from each preparation varied, since as many well labeled cells that were available were analyzed. Analyses were conducted for individual recordings that represented each cell body in this case.

Slice quality was controlled for in three ways: propidium iodide (PI; which is excluded from healthy cells with intact membranes) was washed in after recording granule cells' response to glutamate/DHPG which verified there were no problems with membrane integrity (i.e. the level of glutamate utilized did not seem to compromise cell viability). Separate baseline recordings were taken from an area of the slice different from the ROI before glutamate wash-in to confirm signal stability, and [50mM] potassium chloride was washed into the bath at the end of experiments to confirm the neurons' ability to depolarize and generate a calcium signal (Beani et al., 1994).

2.6 Electrical and Pharmacological Stimulation

Following bath application of the fluorochome, a section of the GCL of cerebellar slices was then imaged using a fluorescence microscopy setup for either: baseline activity, response to [100μM] glutamate, [50μM] DHPG (a potent group 1 mGluR

agonist), or electrical stimulation. Electrical stimulation (Beani et al., 1994; 60 Hz, for 500 ms, at 3.5 μA) occurred twice during a six minute recording at the two and four minute time points with the stimulating electrode placed on afferent mossy fiber projections providing excitatory input to GCs. The stimulation protocol above was chosen because it closely mimics intermittent burst stimulation that GCs would receive *in vivo* (Sola et al., 2004). Both the stimulating and electrodes were made of a section of silver-chloride wire. An additional set of electrical stimulation experiments were conducted with three stimulation points (two, four, and six minutes) over an eight minute recording. Furthermore, [100μM] AIDA (a selective group 1 mGluR antagonist) was washed into the bath during the mid-point stimulation point (four minutes) of the experiment described above. Electrical stimulation success was verified by an extracellular recording electrode approximately 250 μm above the stimulating electrode in the y-plane, next to the particular section of GCL chosen to be imaged. Extracellular recordings were conducted with glass pipettes (1-3 MΩ) filled with a 3-5 micron tip and filled with aCSF.

2.7 Statistical Analysis

ARR Data – Mean latency to fall was calculated for each age x genotype group on each trial and graphed. A one-way between subjects ANOVA was conducted to compare the effect of age on ARR performance. A two-way repeated measures ANOVA (age x trial) was conducted in order to detect effects of age on motor learning. For subsequent analysis, the values from all trials on a given day were averaged to give a single mean for the entire day of trials (i.e. Trials 1-5 on Day 1 were averaged for each animal to give one

overall mean of ARR performance on that day). A Tukey-HSD post-hoc test was used to confirm the ANOVA results.

Paired-sample t-tests were used to compare the pooled data of all groups on Day 1 with that of Day 5 in order to detect significant improvement in motor performance which would be indicative of motor learning (Zlomuzica et al., 2012). Day 5 mean values for all groups were also normalized to what could be called baseline values, on Day 1. This normalization of the data was done using a ratio technique, where Day 5 means were divided by Day 1 means to give a value which is easily comparable even between animals with drastically different levels of ARR performance. All statistics were calculated using SPSS (IBM Inc.) with an alpha level of $p. < 0.05$.

Definitions of Quantification Measures - Quantification measures were calculated with the Igor Pro software package by WaveMetrics (Portland, United States). The software utilizes a user defined baseline (in this case the first ten frames of recordings) and user defined treatment window over which the peak of interest occurs. This time window was defined as 10 frames (Frame rate; Glutamate/DHPG = 5 seconds; Electrical Stimulation/AIDA = 3 seconds) before the agonist wash-in. The treatment window was defined as the start of application up to 10 frames after agonist removal (e.g. in the case of glutamate and DHPG application; frames 20-50). The input time frame, during electrical stimulation, for peak detection was 5 frames before and after the electrical stimulation (i.e. frames 35-45, 75-85, and 115-125). Maximum response was defined as the largest increase in signal amplitude seen over the defined stimulation period.

Area-under-the-curve (AUTC) measurement was included as in some cases the above mentioned quantifications did not give a complete characterisation of a calcium signal. AUTC was calculated by multiplying the sum of the y values (% fluorescence change) by the x-interval (frame rate) for a given recording. As described in Chapter 3 Results, total AUTC measures did not seem to completely describe trends in the recordings where the response appeared bi-phasic. Therefore, in addition to total AUTC being calculated for each recording the calcium response to a particular stimulus was broken into two phases (i.e. the direct response to stimulation and the recovery period after stimulation is ceased) and an AUTC measurement was conducted for each of them. Two phase AUTC measurements were conducted for glutamate and DHPG experiments only.

Data were analysed for significance with a one-way between subjects ANOVA and the Tukey HSD post-hoc test. Data are expressed as mean +/- standard error of the mean (SEM). An alpha level of $p < 0.05$ was set for all statistical analyses.

Chapter 3 Results

3.1 Behavioural Testing

In order to further characterize the ataxia of homozygous animals while testing for motor learning, and to conduct the first known motor testing of heterozygous animals; behavioral testing with the ARR paradigm was undertaken. Animals from our *wdl* colony were divided into different groups based on genotype and PNA. Groups of different ages were included as previous reports had only included young animals (Jiao et al., 2005), and motor performance data for older animals is not present in the literature. Testing was conducted in sets of two trials per day, except for the first day of testing which had five trials. In order to control of physical exhaustion, all animals were given a 45 minute rest period between trials on the same day in their home cage. However, the animals may still have experienced mental fatigue (i.e. boredom) when undergoing trials subsequent to the first on any given day. Data obtained from male and female subjects was not found to be significantly different; therefore, results obtained from both sexes were pooled for analysis.

A five day ARR paradigm was utilized to see if motor learning would be displayed by mutants. As was mentioned previously, motor learning was defined as a significant increase in mean latency to fall on the rota-rod when comparing the first day of trials to the last (Zlomuzica et al., 2012). First, I examined the behavioral data in a broader scope, by comparing different genotypes without breaking up groups by age and by pooling trials by day, which gave a simplified view of overall motor performance in

these groups (Fig. 3.1). Significant motor learning was seen in the WT group, as determined by a paired-sample T-test comparing the pooled performance of all trials on Day 1 to that on Day 5 ($t(15)= -3.99$, $p = .001$), as would be expected. The heterozygous animals performed as well as the WT, except a lack of motor learning was noted, which is represented qualitatively in as their performance plateaus after the trials on day two. In contrast to these two groups, the heterozygote group displayed poor motor performance.

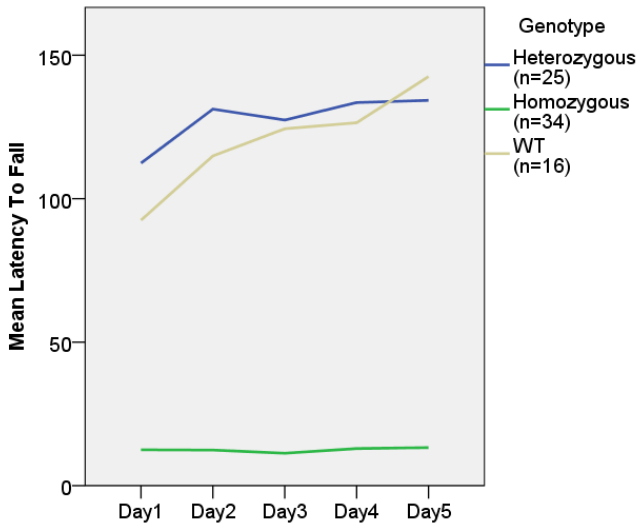

Figure 3.1 – The latency to fall for each day has been pooled, as have the groups at different ages to give an overall view of motor performance. These are the trends which would be expected to be seen based on previous reports of waddles mutants.

In a subsequent analysis, in order to look at the time course of capacity for motor learning across different age groups while controlling for drops in performance during the second trial of a given day that were commonly observed, only the first trials of testing days were compared (Fig. 3.2). Statistical analysis of the data revealed differences in latency to fall to be significant between groups (Day 1 Trial 1 $F(2,65) = 114.89$, $p <$

.0001; Day 5 Trial 1 F (2,65) = 144.50, $p <$ .0001). Post-hoc Tukey-HSD analysis indicated that the homozygous group (D1T1 11.2s ± 2.2; D5T1 12.3s ± 2.0) differed significantly from the WT (D1T1 84.2s ± 6.0; D5T1 133.2s ± 10.3) and heterozygous animals (D1T1 107.4 ± 8.2; D5T1 155.7s ± 10.6; Day 1 Trial 1 $p <$ .0001, .0001 respectively; Day 5 Trial 1 $p <$ .0001, .0001 respectively) as was once again expected. There was no significant difference in performance measured between heterozygous and WT animals; there was also no detectable effect of gender (Wilks' Lambda = .768, F (13,39) = 0.91, p = .555) or age (Wilks' Lambda = .348, F (39,116) = 1.27, p = .161) on rota-rod performance in these two groups. A superior performance was observed in one month old homozygous animals compared with their older cohorts over the last four trials, as detected by a two-way (trial x age) repeated measures ANOVA (Wilks' Lambda = .097, F (35,53) = 1.80, p = .025; Fig. 3.3). Therefore, mutation of Car8 results in age-dependent deterioration in motor performance.

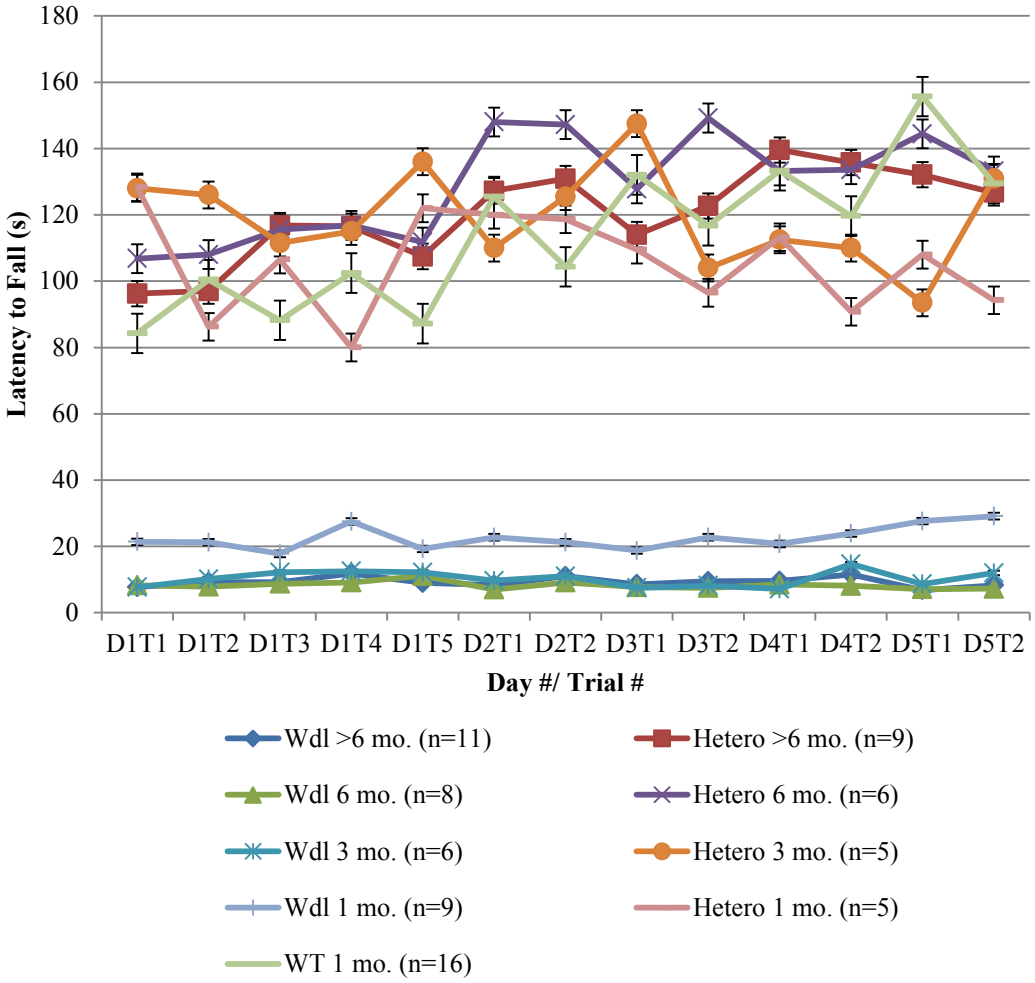

Figure 3.2 – Overall Rota-Rod results obtained from all genotypes across four age points (>6 mo. PNA, 6 mo. PNA, 3 mo. PNA, and 1 mo. PNA; overall n same as table below) except WT which was only tested at one month of age. Males (n=32) and females (n=38) were grouped for this analysis. Bars represent standard error of the mean for each data point. Data is partitioned along the x-axis as means per group on the coded trial and day (e.g. D1T1 represented the first trial on the first day of testing).

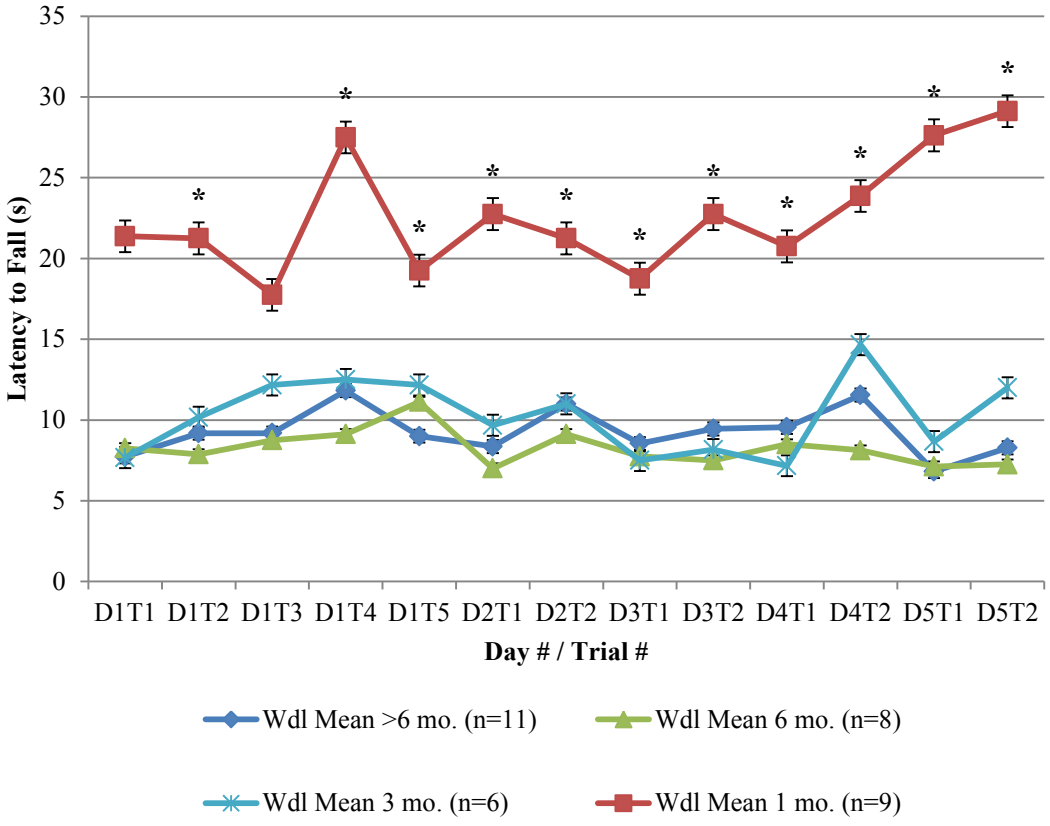

Figure 3.3 – Rota-Rod results for the homozygous group of animals across four age points (>6 mo. PNA, 6 mo. PNA, 3 mo. PNA, and 1 mo. PNA; overall n same as table below). This is from the same data set as the previous figure, but with a different y-scale to show a more detailed view of homozygous groups' data. Bars represent standard error of the mean for each data point. . $p<0.05$*

To examine for evidence of motor learning, mean of results from trials that took place on Day 5 was compared to the overall performance of that group on Day 1. We found that WT displayed significant learning over 5 days, as expected ($t(15)= -7.19$, $p.<.001$). Evidence of motor learning was also seen in the 1 month PNA homozygous group ($t(8)= -5.17$, $p = .001$). Statistical testing for motor learning in the older

homozygous groups, as well as all heterozygous groups, did not reach significance. Normalized data showed that one month old WT and heterozygote animals display similar motor improvements which are not seen in the other group, confirmed with a one-way ANOVA (F (3,29) = 5.68, p = .003) and post-hoc Tukey's test ($p < .01$) (Fig. 3.4).

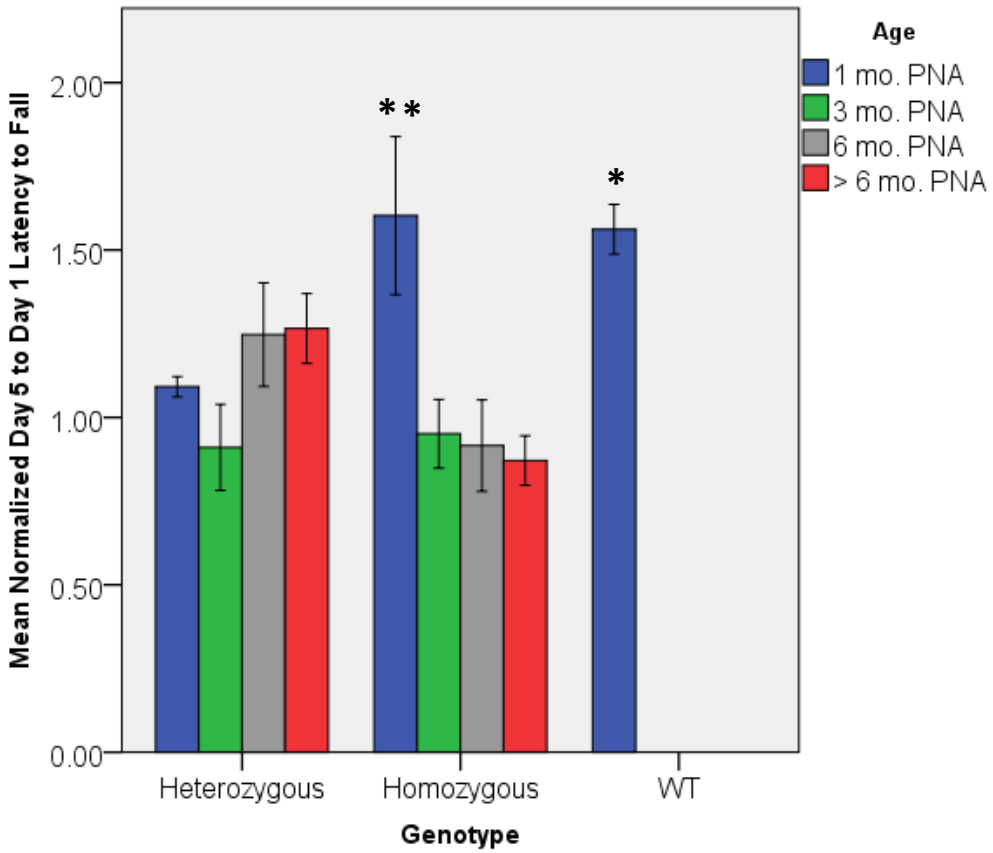

Figure 3.4 – The mean latency to fall of all groups on Day 5 of ARR testing normalized to the mean latency to fall on Day 1. A one-way ANOVA examining genotype (F (2,65) = 7.69, p = .001) found the WT group (n=16) was significantly different from heterozygotes (p.=.028) and homozygotes (p.=.001). Homozygous one month old animals (n=9) show a significant improvement in performance, which was virtually absent in 3mo. PNA (n=6), 6 mo. PNA (n=8), and >6mo. PNA (n=11) groups. This relationship was discovered to be significant with a one-way ANOVA (F (3,29) = 5.68, p = .003)**, and Tukey's HSD test confirmed it is the 1 mo. PNA group (p< .05). There were no significant differences detected between heterozygous groups (>6 mo. PNA, n=9; 6 mo. PNA, n=6; 3 mo. PNA, n=5; 1 mo. PNA, n=5).*

Heterozygous animals had a large amount of variability in their performance over the course of trials which meant motor learning could not be confirmed; in other words, although there were points where heterozygous animals increased their latency to fall in later trials the increase was not always consistent or persistent which may have caused the lack of significance seen in statistical tests. Together with the fact that homozygotes displayed a loss of motor learning ability with age, these results suggest some post-natal developmental effects of the *wdl* mutation which have not been indicated prior to this study. Additionally, the lack of significant motor learning being detected in heterozygous groups brings into question previous reports suggesting that they are free from motor dysfunction and should be used as controls to homozygous *wdl* mice.

3.2 Calcium Imaging

3.2.1 KCl and PI Control Experiments

For Ca^{2+} imaging studies, it is critical to demonstrate that the detected Ca^{2+} signal is not due to compromised cell viability. Bath application of potassium chloride was included to test for cell viability, this was especially important with the potentially toxic dose of glutamate utilized in the first set of experiments. This condition was included to ensure the neurons could still generate a Ca^{2+} response after a recording session. In all reported recordings which had KCl [50mM] exposure prior to agonist application, an appropriate Ca^{2+} response was generated (Toescu, 1999).

As an additional control condition, throughout several experimental conditions, PI was washed into the bath following a typical recording session (Fig. 3.5). Since PI is

known to be taken up by cells with a compromised cellular membrane (Jones & Senft, 1985), it is a good indicator of cell viability (i.e. cells that did not take up PI, can be assumed to have an intact membrane). Wash-in of PI was conducted in the glutamate experimental condition (n=3, animals) and in the DHPG experimental condition (n=3, animals). When the images were overlaid we can see that none of the cells which took up PI took up OG-BAPTA-1-AM (Fig. 3.5 a-c); indicating that cells imaged for calcium levels were viable at the end of recordings. None of the cells which were included in this study's analysis were observed to take up any PI.

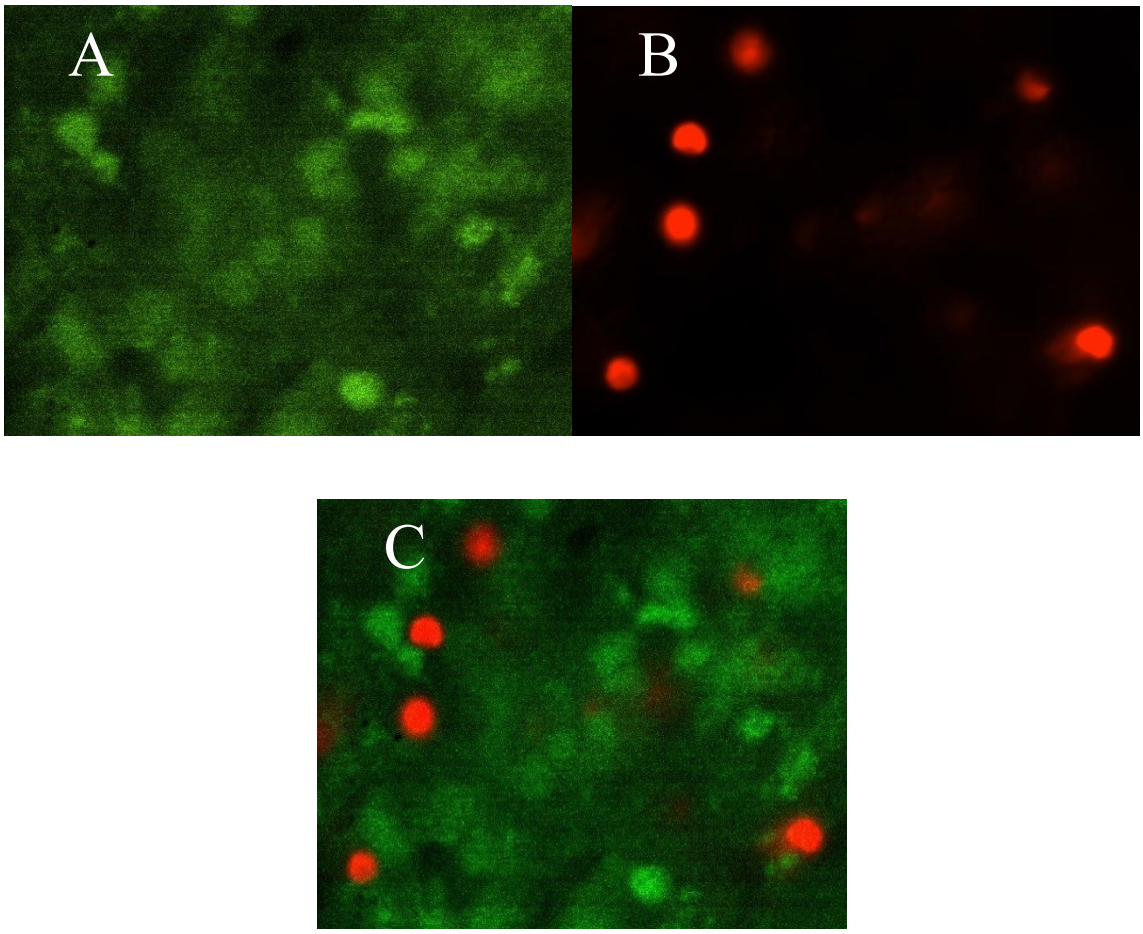

*Figure 3.5 – **A)** Image of the granule cell layer of a typical slice loaded with OG-BAPTA-1-AM. **B)** Image of the same area pictured in part A, but with PI staining following a recording. **C)** An overlay of the two images from previous figure indicating that neurons taking up PI are not the same population that takes up OG-BAPTA-1-AM.*

3.2.2 Glutamate Experiments

Glutamate and its metabotropic receptors, mGluRs, have known connections with CAR8 and IP_3. Therefore, I tested the hypothesis that glutamate-induced Ca^{2+} signaling in GCs is altered in the *Car8* mutation. Animals were divided into groups based on genotype (n=6 for all groups) and GCs from acute vermal slices were imaged.

Qualitatively, an interesting oscillatory pattern was repeatedly observed in WT recordings in response to exogenous glutamate (Fig. 3.6). This pattern is likely a well described oscillatory behavior in populations of GCs that is mediated by timed inhibition from GoCs (Dugué et al., 2009). This pattern was absent in the mutant groups (Figs. 3.7 & 3.8), which displayed Ca^{2+} responses that where abnormal in time-course and magnitude of response.

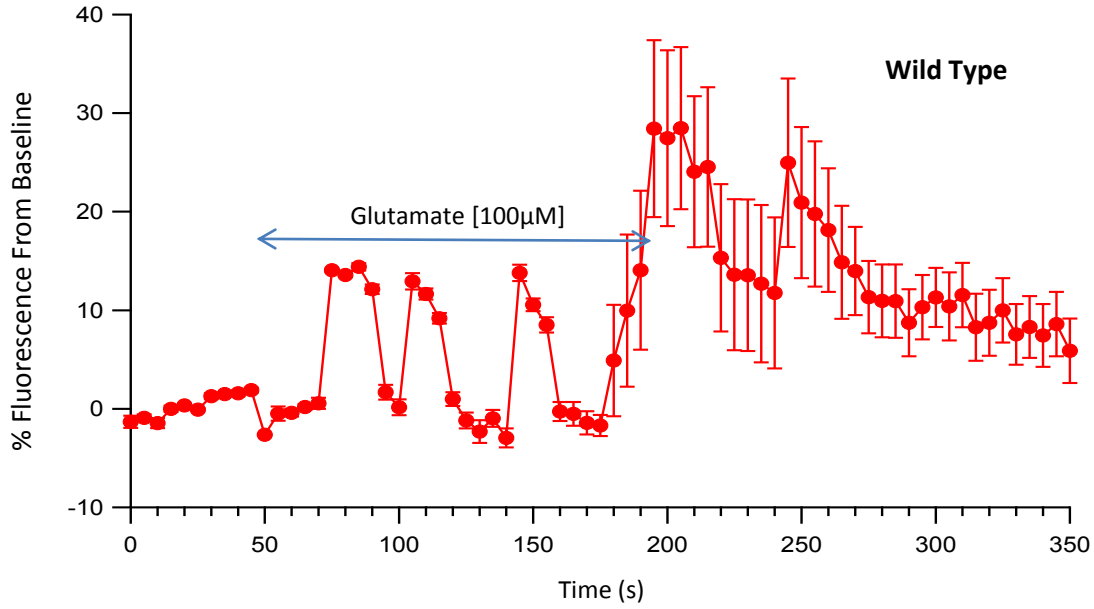

Figure 3.6 - Average trace of wild type granule cell somatic calcium response (% of baseline) to glutamate [100µM] wash-in, n=12 (number of recordings; taken from six different animals). Bars represent standard error of the mean for each data point.

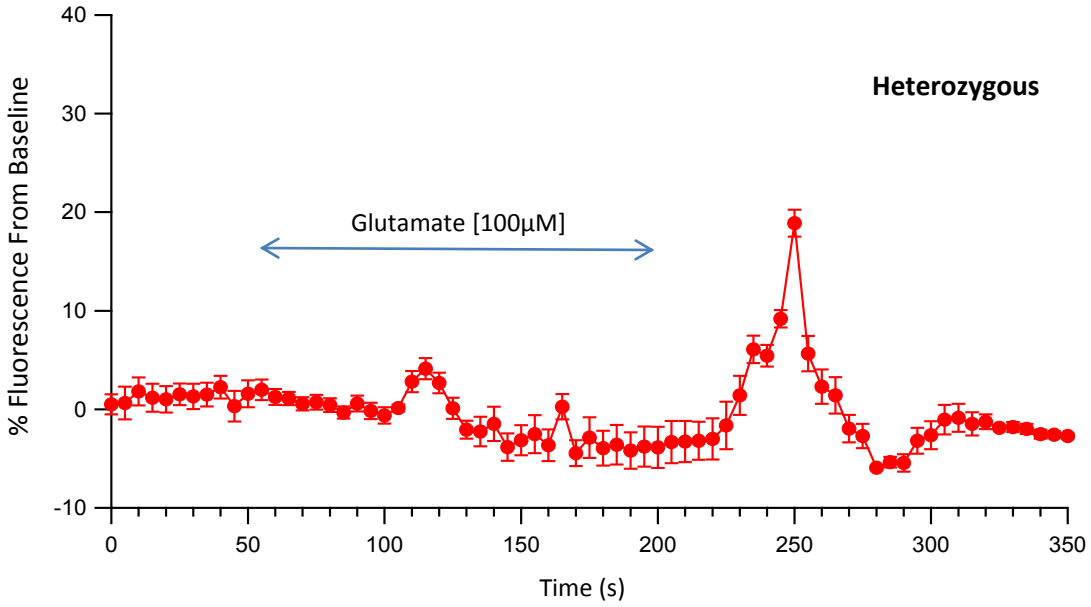

Figure 3.7 - Average trace of heterozygous granule cell somatic calcium response (% of baseline) to glutamate [100µM] wash-in, n=10 (number of recordings; taken from six different animals). Bars represent standard error of the mean for each data point.

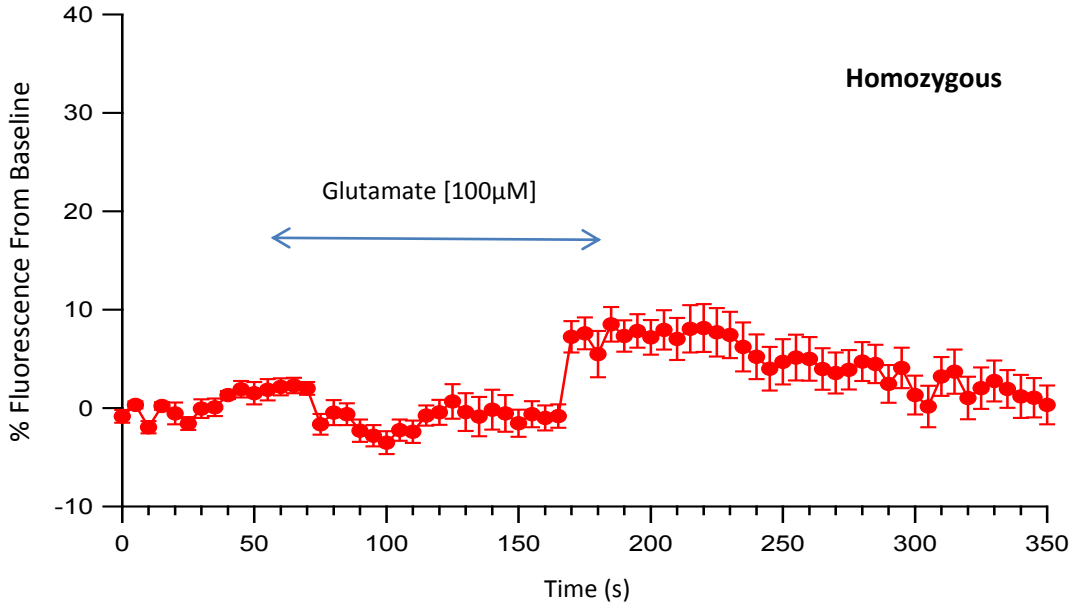

Figure 3.8 – Average trace of homozygous granule cell somatic calcium response (% of baseline) to glutamate [100µM] wash-in, n=10 (number of recordings; taken from six different animals). Bars represent standard error of the mean for each data point.

Maximum response was significantly different between groups (F (2,24) = 3.54, p = .045; Fig. 3.9). Post-hoc analysis with the Tukey-HSD test indicated a significant difference between homozygous and heterozygous/WT animals (p = 0.047) in the maximal response measurement.

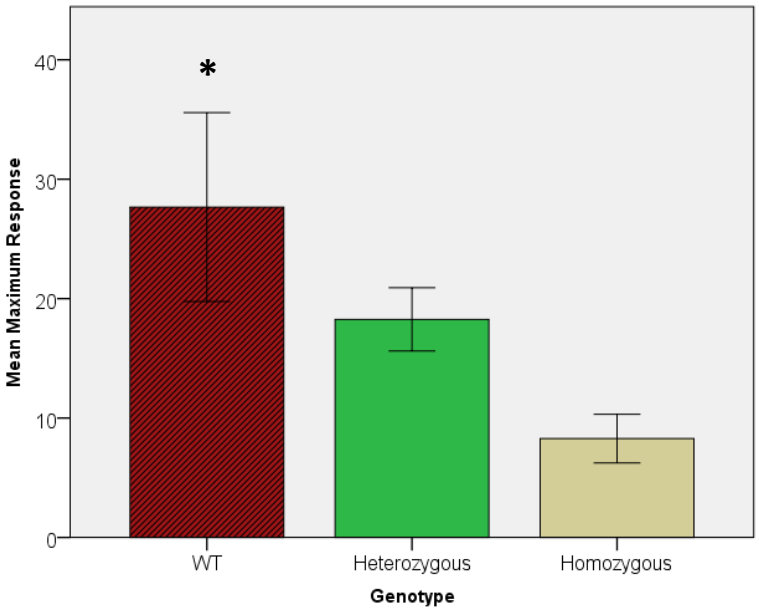

*Figure 3.9 – Mean maximum response values, reported for WT (n=12), heterozygous (n=10), and homozygous (n=10) groups in the glutamate condition. A one-way ANOVA (F (2,24) = 3.54, p = .045), and post-hoc analysis indicated the WT group was significantly different from the mutant groups (p = .047) *. Bars represent standard error of the mean.*

AUTC measurements were conducted in order to better describe aspects of calcium recordings which cannot adequately be described by other quantification methods (i.e. maximum response). As with the previous analysis of this data, the inter-frame time interval is five seconds per frame of imaging. The entire length of each recording was analyzed wholly at first. Analysis indicated a significant difference between groups (F (2,24) = 7.30, p = .003; Fig. 3.10). Post-hoc analysis with the Tukey HSD test indicated the significant difference was between WT and mutant animals (p < .01). Results indicate

that WT animals experienced an overall increase in Ca^{2+} levels in response to glutamate stimulation, while the mutant groups showed little net change. Although there is a clear difference between WT and mutant groups as was expected, the fact that WT had a much greater net increase in Ca^{2+} is perplexing since the lack of functional CAR8 in mutants would theoretically cause more intracellular Ca^{2+} release.

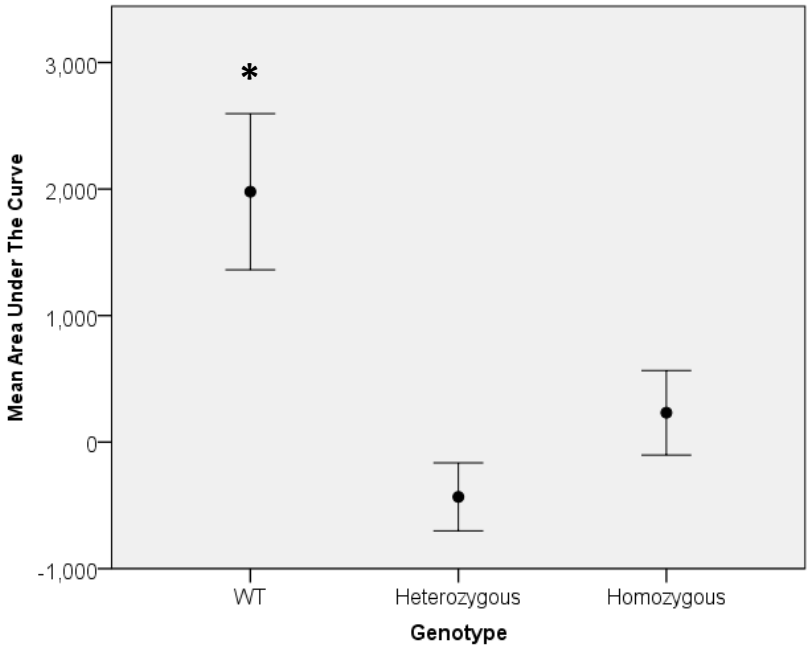

Figure 3.10 – Mean AUTC values of glutamate response in granule cells, reported for WT (n=12), heterozygous (n=10), and homozygous (n=10) groups during glutamate application. A one-way ANOVA (F (2,24) = 7.30, p = .003), and post-hoc analysis indicated the WT group was significantly different from other groups (p < .01). Bars represent standard error of the mean.*

AUTC measures were subsequently divided into two phases for analysis: a phase during glutamate application and another after application ceased. Recordings were split into phases before (50s – 200s) and after (200s – 350s) agonist wash-out of the bath. The reason for this is that the Ca2+ responses appeared biphasic and overall AUTC measurements reported above did not seem to adequately represent the true nature of various calcium recordings. Recordings from both the heterozygous and homozygous groups showed a minor decrease during application followed by a relatively minor increase. The WT group recordings showed an oscillatory pattern during application followed by a large increase in Ca^{2+} following bath wash-out of the agonist.

Relationships between data seen in the overall AUTC measurements (Fig. 3.10) were preserved when the recordings were broken up (Fig. 3.11), however some additional details may be gleaned. The heterozygous animals showed little change between the two phases, as were those obtained for the homozygous group, especially given the relatively high SEM. However, in WT groups there was a considerably larger AUTC measure from the second phase (agonist wash-out) when compared with the first (agonist wash-in). A one-way ANOVA indicated that WT animals were significantly different from mutant groups with respect to both the first (F (2,24) = 6.75, p = .007) and second (F (2,24) = 6.15, p = .010) phases of the calcium signal, confirmed by post-hoc Tukey's HSD.

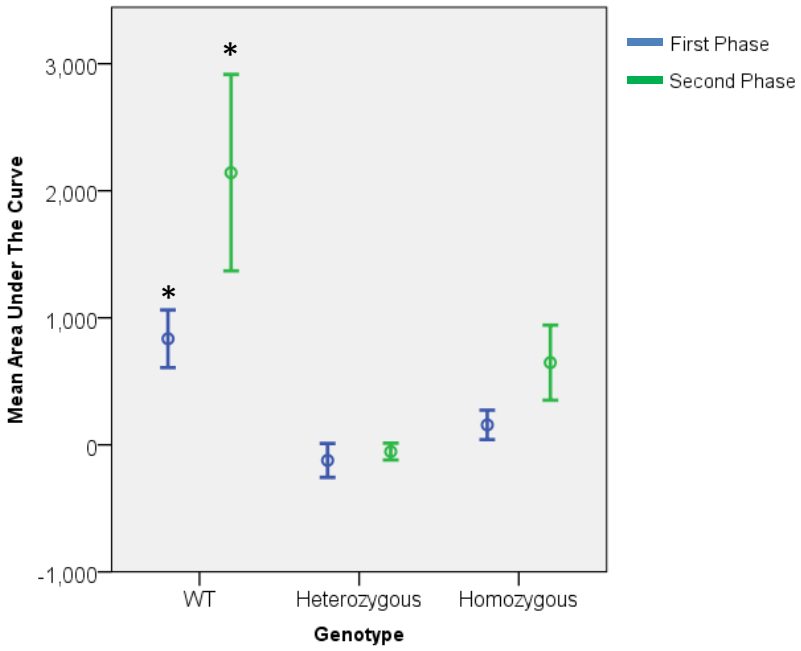

*Figure 3.11 – A breakdown of the previous figure, this image depicts mean AUTC values obtained when calcium recordings were broken into two phases (First Phase 50s-200s & Second Phase 200s-350s). These are values from granule cell recordings, reported for WT (n=12), heterozygous (n=10), and homozygous (n=10) groups in the glutamate condition. One-way ANOVA confirmed that the WT group was significantly different from the mutant groups during the first ($F(2,24) = 6.75$, $p = .007$) and second ($F(2,24) = 6.15$, $p = .010$) phases of the calcium signal. Bars represent standard error of the mean, * $p. < .01$.*

3.2.3 DHPG Experiments

In order to specifically characterize the group I mGluR contribution to observed calcium responses, a set of experiments utilizing the selective group I mGluR receptor agonist DHPG were conducted. A gradually increasing response was seen from the WT group as might be expected given the generally slower response of the metabotropic receptors. Both of the mutant groups showed responses that were much different than the WT mice. The homozygous group showed a response similar to WT animals, with a brief peak after agonist exposure and a gradually declining fluorescent signal afterwards. Homozygous animals showed a relatively large increase in Ca^{2+} levels (Fig. 3.14), when compared to the maximal response seen in wild type animals (Fig. 3.12).

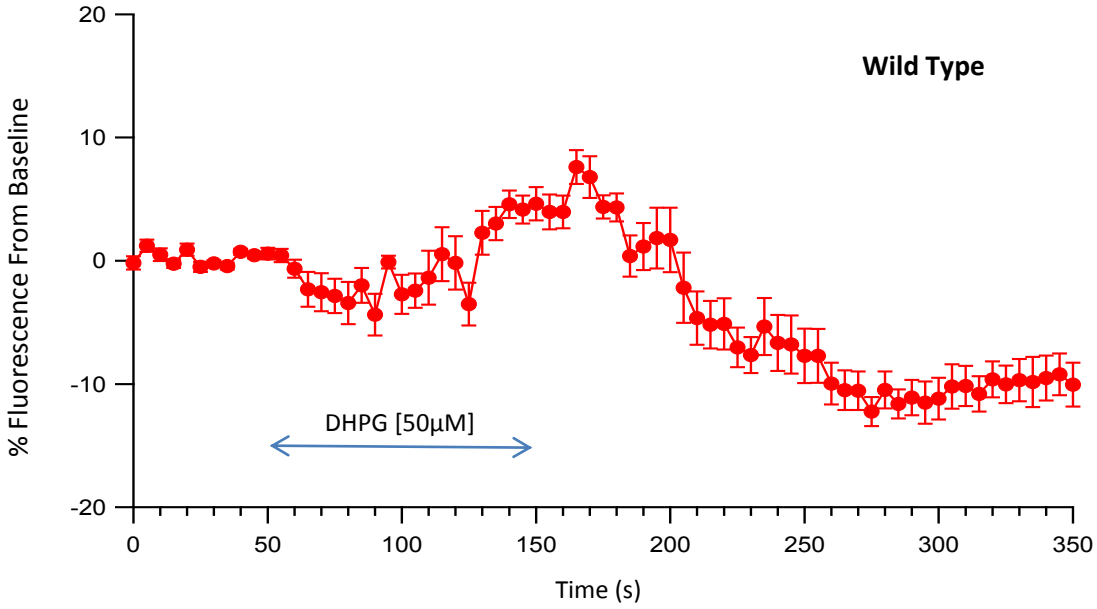

Figure 3.12 - Average trace of wild type granule cell somatic calcium response (% of baseline) to DHPG [50µM] wash-in, n=12 (number of recordings from five different animals). Bars represent standard error of the mean for each data point.

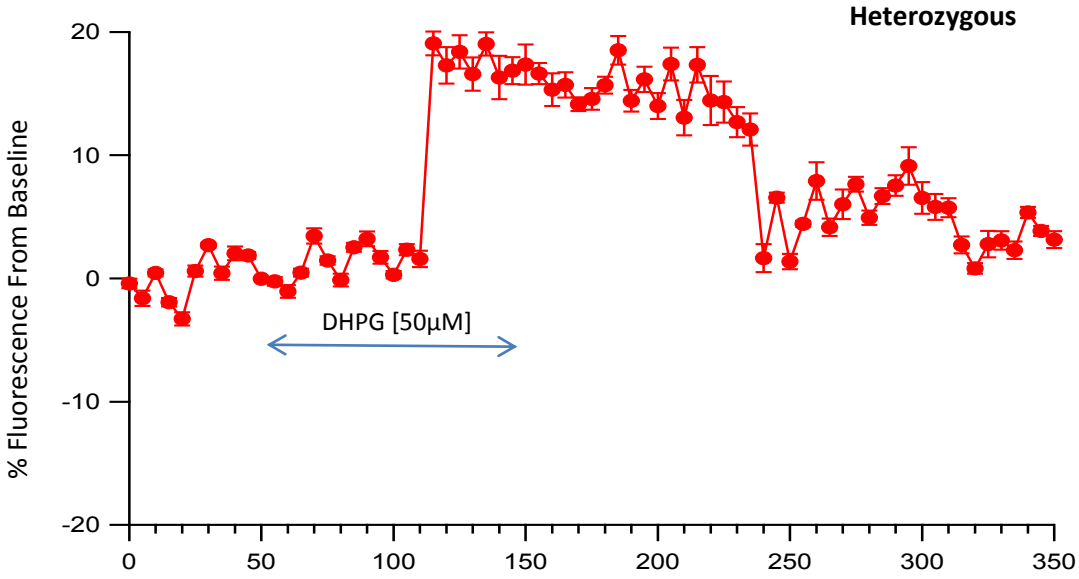

Figure 3.13 - Average trace of heterozygous granule cell somatic calcium response (% of baseline) to DHPG [50µM] wash-in, n=9 (number of recordings from five different animals). Bars represent standard error of the mean for each data point.

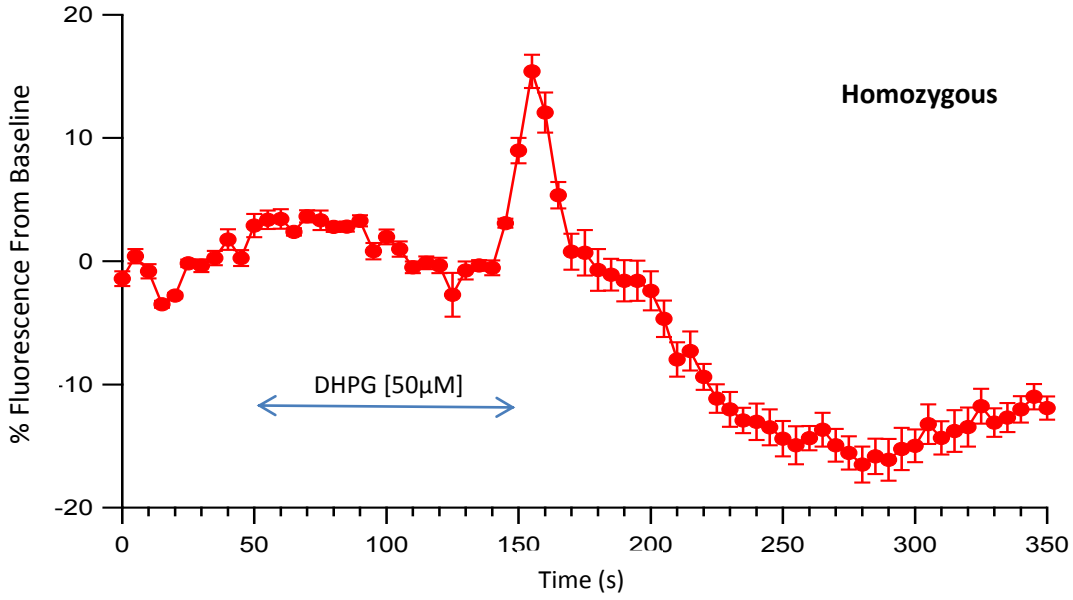

Figure 3.14 - Average trace of homozygous granule cell somatic calcium response (% of baseline) to DHPG [50µM] wash-in, n=15 (number of recordings from five different animals). Bars represent standard error of the mean for each data point.

Interestingly, the largest Ca^{2+} response was seen in heterozygous animals (20.57% ± 2.08, n=9), followed relatively closely by homozygous animals (15.29% ± 2.54, n=15). A comparatively small increase was seen in the WT group (7.96% ± 2.14, n=12). These results were significant (F (2,35) = 5.52, p = .009), and a post-hoc Tukey HSD test indicated differences between WT and Heterozygous groups (p = .008), as well as Heterozygous and Homozygous groups (p = .026).

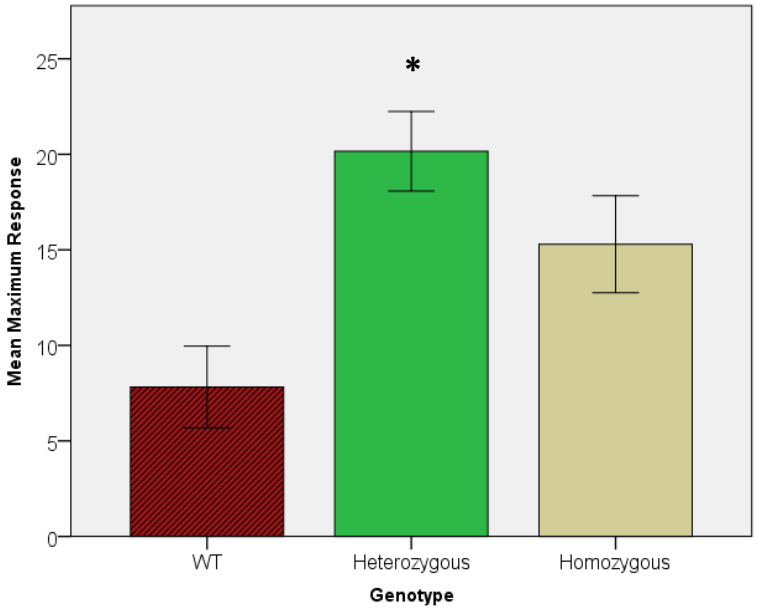

Figure 3.15 – Mean maximum response of granule cell somatic calcium signal in response to DHPG [50μM] wash-in; reported for homozygous (n=15), heterozygous (n=9), and WT recordings (n=12). Bars represent standard error of the mean (n=5 animals). p< 0.05 as detected by a one-way ANOVA.*

As in the glutamate experiment, AUTC measures were first taken for entire recordings as a whole. Analysis of AUTC measurements indicated a significant difference between groups (F (2,35) = 27.12, p = .0001). Post-hoc analysis with the Tukey HSD test

indicated the significant difference was between heterozygous animals and the homozygous and WT groups ($p < .001$), as can be seen in Figure 3.16. WT and homozygous animals experienced an overall net depression of Ca^{2+} levels in response to DHPG, while the heterozygous groups showed a net increase. This was expected as the average tracing of heterozygotes (Fig. 3.13) shows a much longer increase in Ca^{2+} levels than is seen in the other groups.

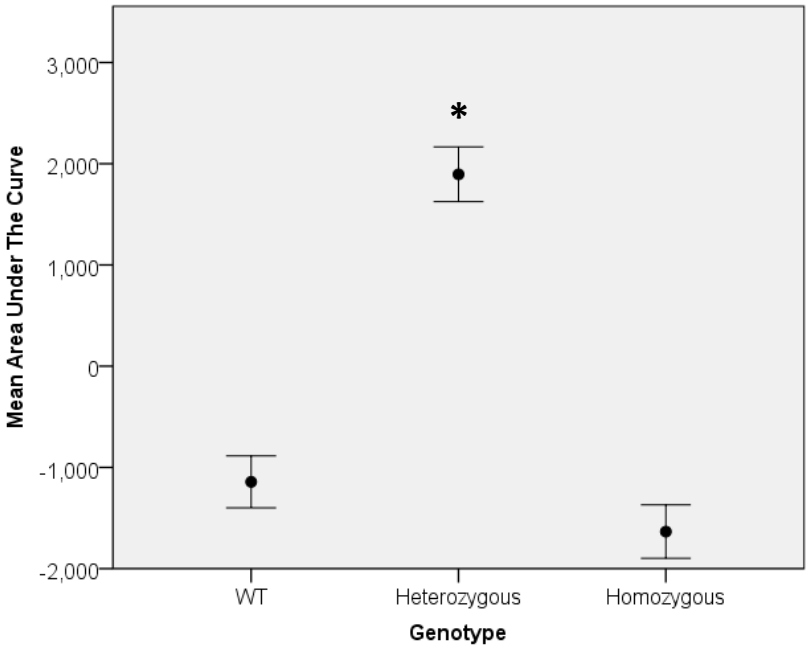

*Figure 3.16 - Mean AUTC reported for the granule cell layer of WT (n=12), heterozygous (n=9), and homozygous (n=15) groups in the DHPG condition. One-way ANOVA revealed a significant difference (F (2,35) = 27.12, p < .0001), and post-hoc analysis indicated it was heterozygous groups versus WT and homozygous groups that was significant (p < .001). Bars represent standard error of the mean, * p. < .01.*

Breakdown of AUTC measurements into two phases (Fig. 3.17) yielded some interesting insights into trends which cannot be seen in the overall measures (Fig. 3.16). Heterozygous groups are still show a significantly higher AUTC measure during the first (F (2,35) = 34.79, p < .0001) and second (F (2,35) = 26.64, p < .0001) phases of

recordings: This was confirmed with Tukey's HSD ($p < .0001$). An interesting relationship which was revealed by the breakdown analysis is that in both WT and Homozygous animals there was little overall change in calcium signal during the first phase of recording but in the second phase there is a large drop in amplitude (Fig. 3.16). This finding coincides well with the patterns seen in the average DHPG condition recordings, where a drop in signal amplitude can easily be seen after the agonist is washed out of the bath in WT and Homozygous groups (Figs. 3.12 & 3.14).

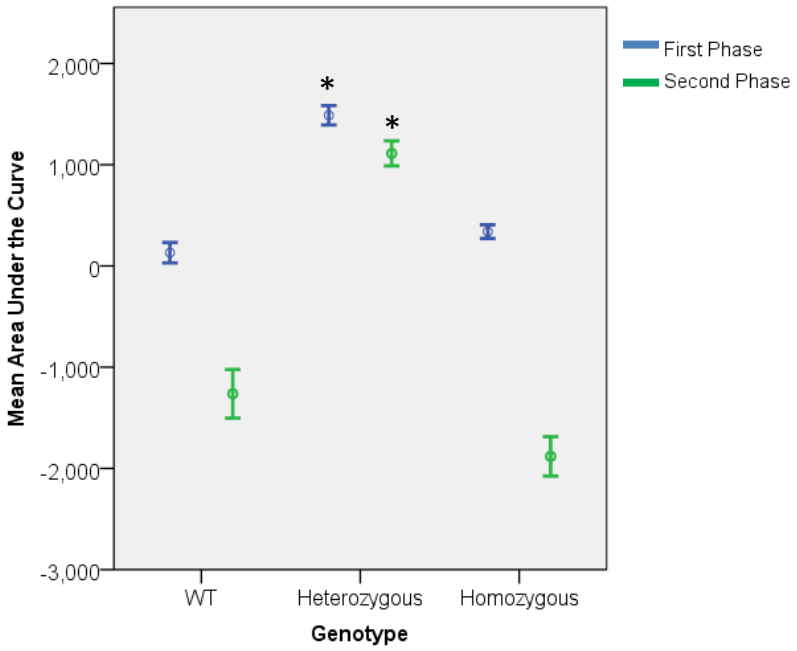

*Figure 3.17 – A breakdown of the previous figure, this image depicts mean AUTC values obtained when calcium recordings were broken into two phases (First Phase 50s-200s & Second Phase 200s-350s). These are values from granule cell recordings, reported for WT (n=12), heterozygous (n=9), and homozygous (n=15) groups in the DHPG condition. One-way ANOVA confirmed that the heterozygous group was significantly different from the WT and homozygous groups during the first ($F(2,35) = 34.79$, $p < .0001$) and second ($F(2,35) = 26.64$, $p < .0001$) phases of the calcium signal. Tukey's HSD confirmed that it is the heterozygous groups that are significantly different ($p < .0001$). Bars represent standard error of the mean, * p. < .0001.*

3.2.4 Electrical Stimulation Experiments

To elucidate the role of CAR8 in excitatory synaptic transmission, electrical stimulation was chosen as it allows precise control over stimulus length, strength, and timing of excitatory synaptic activity and will provide results closer to those that would be observed *in vivo.* Averaged tracings of granule cell Ca^{2+} to electrical stimulation of afferent MFs (60 Hz, 500 ms) are provided below for WT (Fig. 3.18; n=8), heterozygous (Fig. 3.19; n=9), and homozygous (Fig. 3.20; n=9) groups.

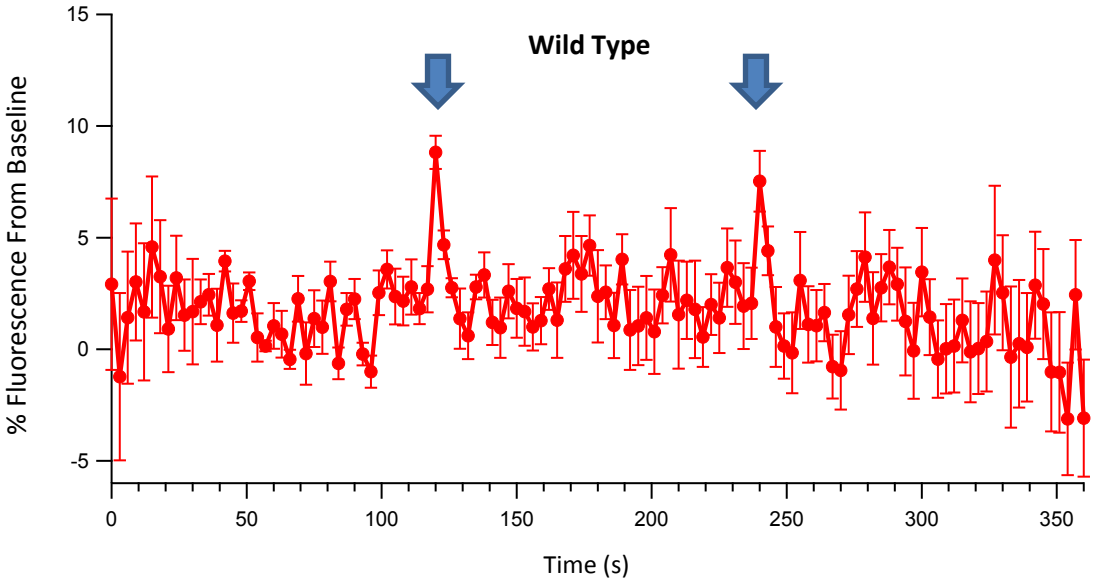

Figure 3.18 - Average trace of wild type granule cell somatic calcium response (% of baseline) to electrical stimulation (3.5 µA, 60 Hz, 500ms) at two time-points (120s & 240s) , n=8 (number of recordings from three different animals). Bars represent standard error of the mean for each data point. Arrows indicate times of electrical stimulation.

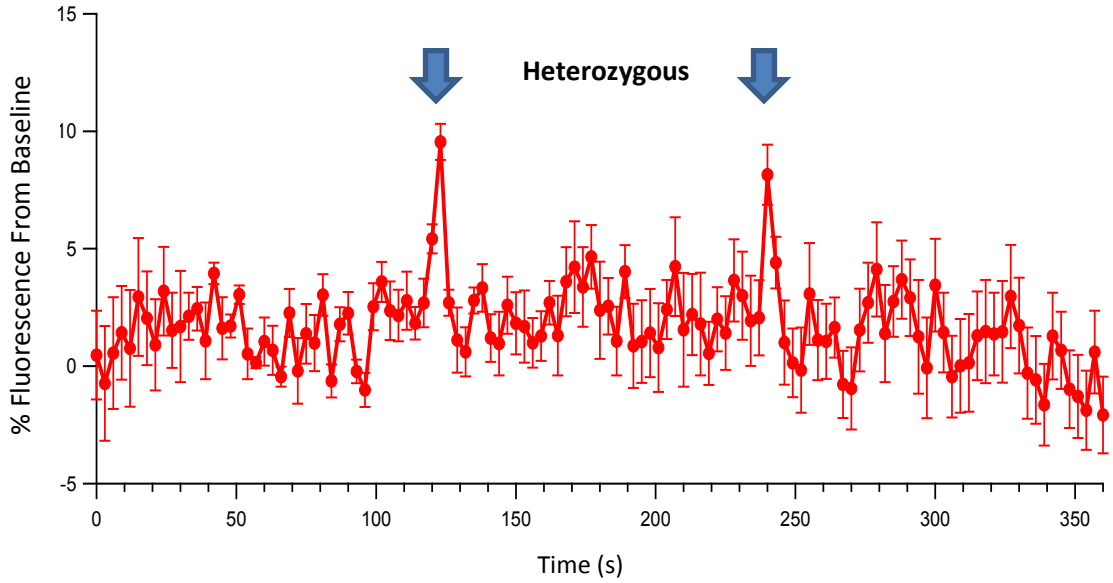

Figure 3.19 - Average trace of heterozygous granule cell somatic calcium response (% of baseline) to electrical stimulation (3.5 µA, 60 Hz, 500ms) at two time-points (120s & 240s), n=9 (number of recordings from three different animals). Bars represent standard error of the mean for each data point. Arrows indicate times of electrical stimulation.

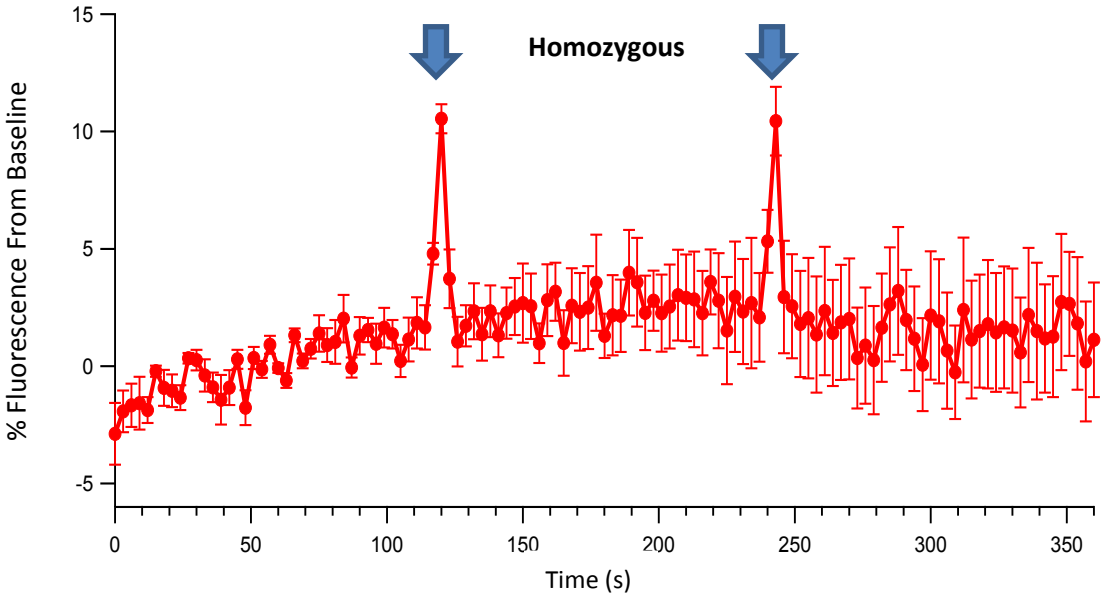

Figure 3.20 - Average trace of homozygous granule cell somatic calcium response (% of baseline) to electrical stimulation (3.5 µA, 60 Hz, 500ms) at two time-points (120s & 240s) , n=9 (number of recordings from three different animals). Bars represent standard error of the mean for each data point. Arrows indicate times of electrical stimulation.

AUTC measurement was once again conducted to discern if there was any difference in the overall output (either positive of negative) of the recorded calcium signal. As with the previous analysis of this data, the inter-frame time interval is five seconds per frame of imaging. AUTC analysis for the electrical stimulation set of experiments yielded non-significant, with WT (Mean= 603.5 ± 290.72), heterozygous (Mean=584.7 ± 324.6), and homozygous (Mean=916.6 ± 389.5) groups showing little difference between them (Fig. 3.21). Statistical testing with a one-way ANOVA revealed no statistically significant differences between groups.

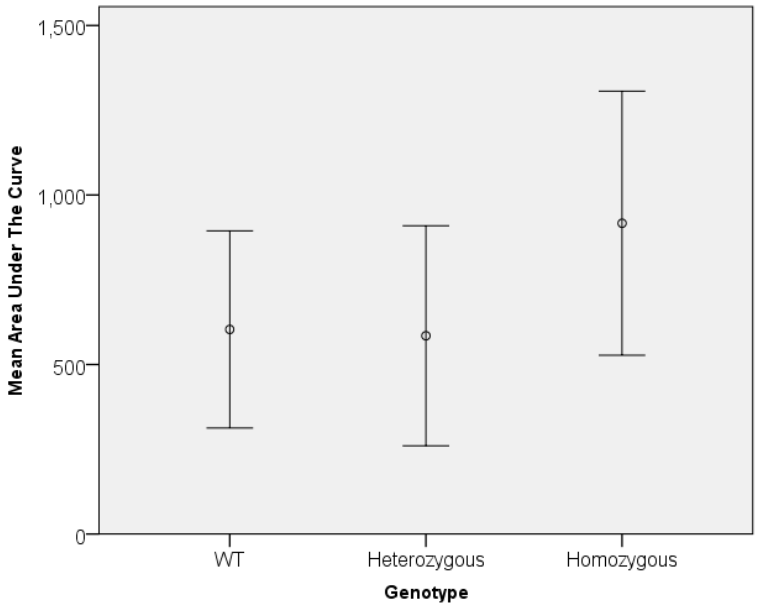

Figure 3.21 – Mean AUTC reported for the granule cell layer of WT (n=8), heterozygous (n=9), and homozygous (n=9) groups in the electrical stimulation condition. Bars represent standard error of the mean.

Slices were stimulated twice to observe whether plasticity at the MF-GC synapse would occur or not with a stimulation paradigm known to have the potential to induce LTD and LTP of this synapse under different conditions (Bianchi et al., 1992; Beani et al., 1994; Gall et al., 2005). There was no significant difference detected when comparing the amplitude of the first and second responses to electrical stimulation in any group (Fig. 3.22); indicating there was no change in the strength of Ca^{2+} response experienced at the cell soma as a result of stimulation induced MF-GC LTP.

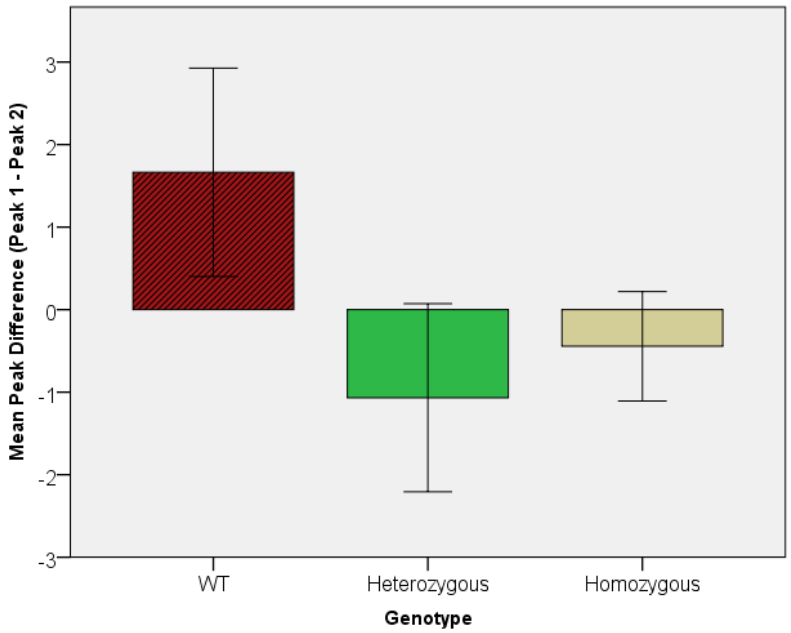

Figure 3.22 – Mean maximum response difference between the first and second peak of granule cell somatic calcium signal in response to electrical stimulation; reported for homozygous (n=9), heterozygous (n=9), and WT recordings (n=8). Bars represent standard error of the mean.

3.2.5 Electrical Stimulation & AIDA Experiments

Coupling electrical stimulation with temporary bath application of the $mGluR_1$ antagonist AIDA allowed the relative contribution of group I mGluRs to a typical Ca^{2+}

response to synaptic stimulation to be determined. Application of AIDA reliably reduced the amplitude of response to MF electrical stimulation in all groups (Figs. 3.23, 3.24, 3.25); an effect which was reversed upon wash-out. The largest decrease in amplitude was seen in homozygous animals (35.03%; n=8; SEM=1.71), than WT (28.29%; n=9; SEM=6.37) and wild type animals (25.38%; n=8; SEM=3.37), compared to the first stimulation peak in the given recording. These differences between groups were determined to not be statistically significant (F (2,24) = 1.49, p = 0.26). The lack of significance may be due to the relatively low number of subjects in this set of experiments.

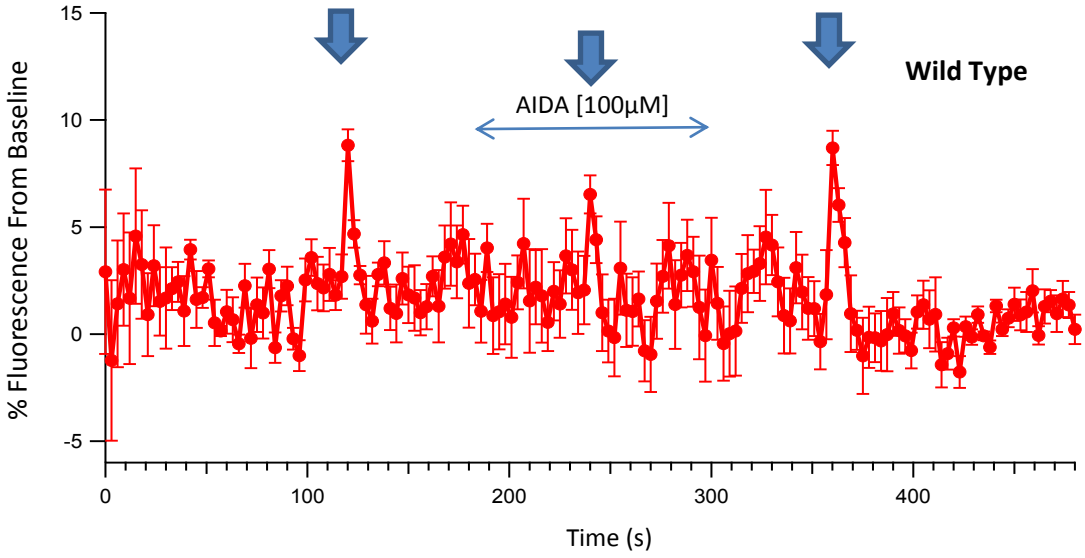

Figure 3.23 - Average trace of wild type granule cell somatic calcium response (% of baseline) to electrical stimulation (3.5 µA, 60 Hz, 500ms) at three time-points (120, 240, & 360 seconds) with AIDA [100µM] washed into the bath from 180 until 300 seconds. n=9 (recordings from three different animals); bars represent standard error of the mean for each data point. Arrows indicate times of electrical stimulation.

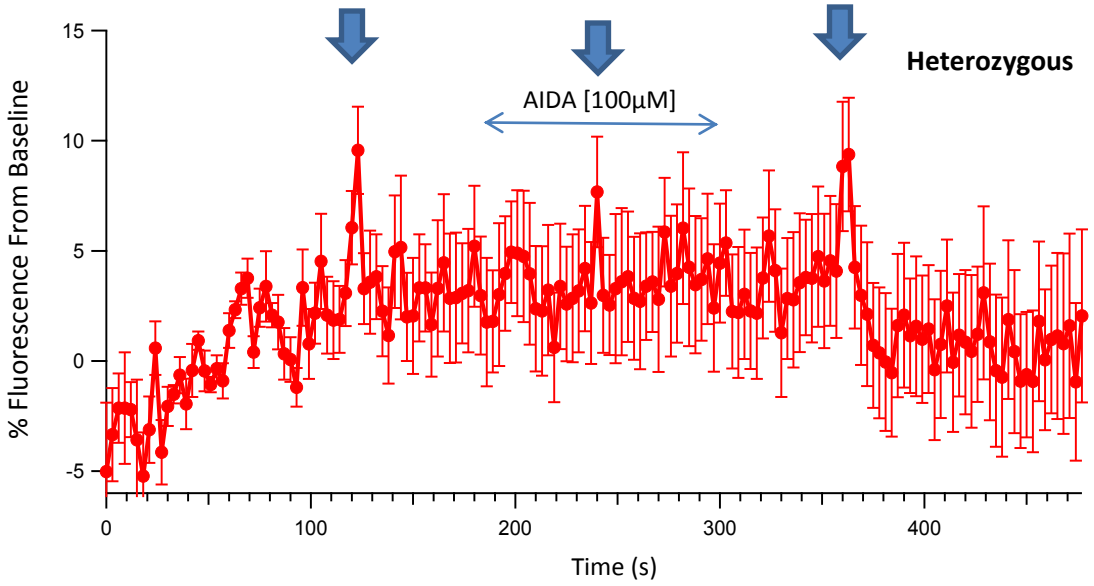

Figure 3.24 - Average trace of heterozygous granule cell somatic calcium response (% of baseline) to electrical stimulation (3.5 µA, 60 Hz, 500ms) at three time-points (120, 240, & 360 seconds) with AIDA [100µM] washed into the bath from 180 until 300 seconds. n=8 (recordings from three different animals); bars represent standard error of the mean for each data point. Arrows indicate times of electrical stimulation.

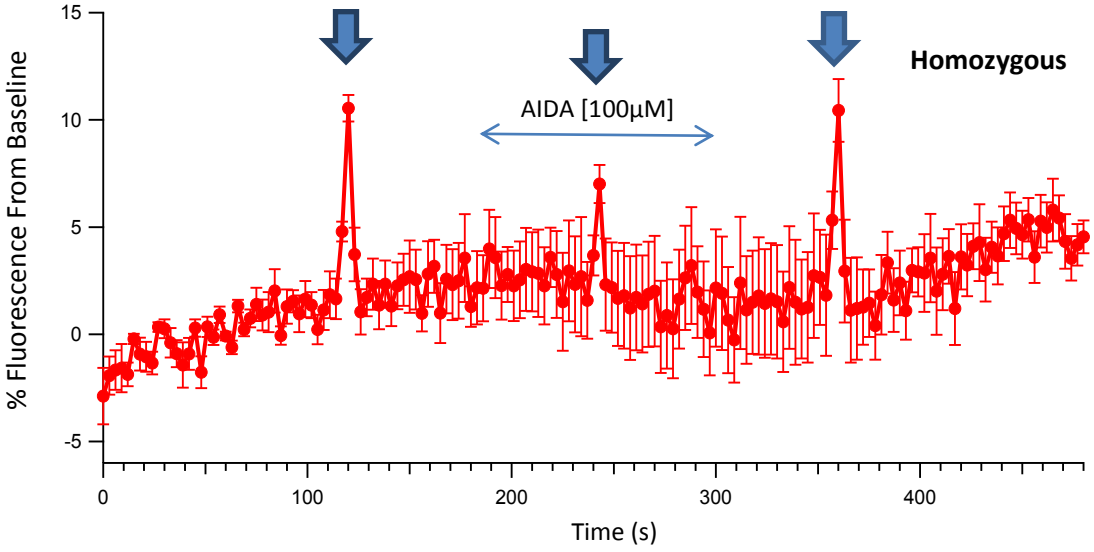

Figure 3.25 - Average trace of homozygous granule cell somatic calcium response (% of baseline) to electrical stimulation (3.5 µA, 60 Hz, 500ms) at three time-points (120, 240, & 360 seconds) with AIDA [100µM] washed into the bath from 180 until 300 seconds. n=8 (recordings from three different animals); bars represent standard error of the mean for each data point. Arrows indicate times of electrical stimulation.

Homozygous animals would theoretically be thought to have the largest decrease with group 1 mGluR blockade, but this was not seen. These differences in peak response were not significantly different between genotypes, as determined by a one-way ANOVA (Fig. 3.26). All groups of animals maintained a steady baseline throughout recordings, and there were also no significant differences between the maximal response of the first and third peak in recordings.

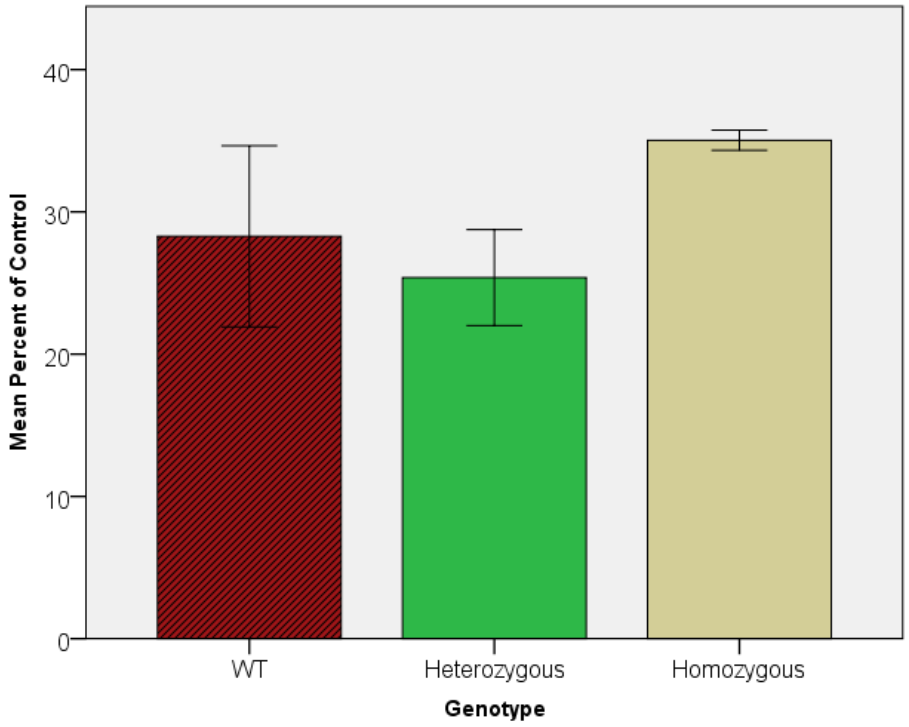

*Figure 3.26 – Graph comparing the mean percent of control between groups, which was defined as (((Peak 1 – Peak 2)/Peak 1) * 100). There were no significant differences between WT (n=9), heterozygous (n=8), and homozygous (n=8) groups. Bars represent standard error of the mean*

AUTC analysis from the AIDA/electrical stimulation experiments yielded results that were not significant, with WT (M= 825.6 ± 247.0), heterozygous (M=584.9 ± 844.6), and homozygous (M=987.47 ± 623.1) groups showing little difference between them.

Both the AUTC results for this set of experiments, and the electrical stimulation experiments without AIDA yielded insignificant data. This is likely due to the relatively high level of background 'noise' in the recorded Ca^{2+} signal in these cases causing a very large standard deviation in all groups. Although these experiments did produce significant data regarding response dynamics in their current form, an increased n in these conditions may lead to a significant AUTC finding.

Chapter 4 Discussion

It was originally hypothesized that the CAR8 mutation significantly altered Ca^{2+} dynamics in the cerebellum. This was thought to be mediated by a loss of inhibition of IP_3 binding to the IP_3R, since the only known function of CAR8 is to inhibit IP_3 binding to its receptor. Within the bounds of this hypothesis only the homozygous animals would have disturbed neuronal signaling as only they displayed ataxia. Conversely, according to this hypothesis heterozygous animals should therefore have neuronal Ca^{2+} within normal limits. However, we demonstrate that heterozygous animals also have disturbed Ca^{2+} dynamics and also display impaired motor learning. Altered Ca^{2+} dynamics may cause a difficulty with motor learning in homozygous and heterozygous groups. Additionally, the alterations in Ca^{2+} signaling recorded did not completely match up with theoretical predications based on the hypothesis. Possible candidates causing this deviation from the predicted state include: compensatory mitochondrial Ca^{2+} sequestration, morphological changes in response to chronically altered Ca^{2+} signaling from birth in the *wdl* mice, and/or a biphasic response of GCs to the altered levels of $[Ca^{2+}]_i$. These possibilities are discussed further below along with other interesting features of the collected data.

There were significant differences between the Ca^{2+} signaling of homozygous mutant *wdl* mice and their WT counterparts (e.g. Figs. 3.9 & 3.18). Results obtained while using DHPG are more pertinent since the known action of CAR8 is on the IP_3 pathway, which is affected directly by group 1 mGluRs (Hirota et al., 2003). Subsequent experiments utilizing electrical stimulation of afferent GCL connections in tandem with a group 1 mGluR antagonist, AIDA, both confirmed and extended our basic hypothesis that

there is altered Ca^{2+} signaling in the cerebella of *wdl* mice. This extension is that heterozygous *wdl* mice also experience altered Ca^{2+} signaling and that contrary to previous reports do experience motor difficulties in the form of impaired motor learning.

4.1 Involvement of the CAR8 Mutation in Motor Coordination and Learning.

4.1.1 Rota-Rod Experiments

Behavioral testing on the rota-rod apparatus was undertaken to further characterize the ataxic phenotype of both homozygous and heterozygous *wdl* mice (Monville, Torres, & Dunnett, 2006). Homozygous mutants showed a significant age-linked difference in latency to fall from the rota-rod apparatus (Fig. 3.1). When homozygous subjects were examined at one month of age they performed significantly better than three or six month PNA homozygous cohorts (Fig. 3.2). Significant ARR results may be partially attributable to a difference in body mass between homozygous groups of different ages affecting the ease of balancing. This could not be analyzed with a post-hoc correlational study however, as the weights of mice were not recorded for this experiment. This difference in latency to fall indicates that calcium imaging experiments conducted in older versus younger homozygous *wdl* mice may yield significantly different data. This was not conducted in this study as neural tissue from older animals is more sensitive to physiological perturbations during experimentation and generally loads calcium indicator much less effectively.

Although one month old homozygous animals preformed significantly worse than heterozygotes and WT groups of any age, their outperformance of older subjects with the

same genetic background suggests the ataxia is present at birth and that it worsens during the first several weeks of life. It may be that the absence of functional CAR8 affects prenatal development as well as further postnatal development and synapse maintenance. Compared to rota-rod testing conducted by Jiao et al., (2005), the results obtained here indicate a much lower latency to fall. This can be accounted for by the different methodologies employed; Jiao et al., (2005), utilized a fixed speed rota-rod paradigm, whereas we choose the ARR paradigm mentioned previously. The ARR paradigm more accurately characterizes the differences between mutant ataxic mice whereas the alternative fixed speed rota-rod paradigm better characterizes motor impairments due to drug exposure (Rustay et al., 2003). Additionally, the current experiment included the heterozygous group and conducted multiple trials over five days; Jiao et al., (2005) only conducted three trials spaced over the same day which did not allow for motor learning to be investigated.

Motor learning was previously defined as significant improvement in the pooled mean of the first day of trials (i.e. five trials total) when the same group was tested on the final two days of the ARR (i.e. two trials per day, four total). A clear trend of increasing latency to fall over the course of the trials was only seen in the one month old homozygous animals and in the WT group which were each determined to have displayed motor learning. Motor learning in the one month old homozygous group was established by using a two-way repeated measure ANOVA (time of trial x age) over the last four trials (Fig. 3.2). The results from this ANOVA also confirmed that it was the youngest (1 mo. PNA) homozygous animals who significantly improved their motor performance over time.

As further evidence for motor learning, average latency to fall on Day 5 was normalized to average data from Day 1 for all rota-rod groups individually (Fig. 3.3). These results agreed with the ANOVA conducted previously, that motor learning was displayed by the 1 month PNA homozygous and WT groups. There were varying degrees of improvement in the latency to fall, as denoted by a greater normalized value, of heterozygous animals, but not to the extent of young homozygotes and WT mice. This lack of consistency in motor performance was only seen in the heterozygous groups; the homozygous groups either performed consistently poorly or in the case of the one month old homozygotes, performed consistently until there were persistent improvements. It seems odd at first that young heterozygous animals did not display motor learning, as the 1 mo. PNA group of the other genotypes did. However, it may be that calcium dynamics are further disturbed in young heterozygous animals than in homozygous cohorts since alterations in the timing of neuronal firing is known to affect motor learning; whereas ataxic symptoms (i.e. those seen in homozygous mutants) are more generally linked to morphological abnormalities of the cerebellar cortex (Schonewille et al., 2007).

4.1.2 Rota-Rod Experimental Limitations

With any behavioral methodology there is the recurring issue of large amounts of variability in subjects' behavioral performance. Variability in performance can be due to numerous factors including, but not limited to, environmental conditions (i.e. time of day of testing, air pressure, and temperature) and inherent personality variability in subjects (i.e. aggressiveness, sociability, and introversion). This is normally controlled for by large sample sizes where outlying data points from subjects are compensated for by being

grouped with those from subjects performing in the normal range, when calculating the means. This is why the minimum number of subjects per group in this experiment was 15, and although this helped us to obtain significant results, the inherent variability in behavioral research could still be affecting the results obtained from statistical analysis.

4.2 Granule Cell Calcium Signaling in Response to Several Stimulation Paradigms

4.2.1 Glutamic Acid Application Experiments

The first set of imaging experiments were conducted with the excitatory neurotransmitter glutamate as it provides general excitation to neuronal systems *in vivo* (Robinson & Coyle, 1987) and is known to stimulate cerebellar GCs. It was expected that heterozygotes would show results similar to WT since they do not display a behavioral phenotype, however, this was not the case. WT animals had a much larger maximum Ca^{2+} response to glutamate stimulation than homozygous *wdl* mutants. Heterozygous animals' maximum response was in between the values from the other two genotypes, but overall closer to the WT response. Differences in the amount of Ca^{2+} response and the speed of that response would have direct functional implication in the GCL. As mentioned earlier the presence of higher or lower $[Ca^{2+}]_i$ drives plasticity either towards LTD or LTP in both the MF-GC and GoC-GC synapses (Gall et al., 2005). Disturbing the balance of 'opposing forces' in plasticity at one of the major input areas into the cerebellum would affect signaling in the entire cerebellar circuitry. As the importance of the GCL in modulating known motor programs was recently postulated

(D'Angelo & De Zeeuw, 2008), these alterations in Ca^{2+} signaling may also affect accurate modulation of stored motor programs.

Qualitative comparison of average tracings from WT and homozygous mutants' yielded an interesting observation. The average tracing from the WT group (Fig. 3.6) shows clear oscillations of Ca^{2+} during glutamate application in GCs which is quite uniform and has a very low SEM. This pattern likely reflects the well described GC population oscillation in excitability which is mediated by concurrent activation of GoCs that provide inhibitory input (Dugué et al., 2009). As the GC population is excited by bath applied glutamate, GoCs are also stimulated to provide inhibitory input postulated to control GCs from becoming overstimulated and contributes to their information processing abilities (Ito, 2006). The pattern dissipates later in the recording, near the end of glutamates time in the bath, which seems to reflect the GoCs ability to provide feed-back inhibition and maintain the oscillatory pattern being overwhelmed by the strong excitation provided by the exogenous glutamate application. Homozygous mutants however, have a tracing that shows similar patterns, but lacks the uniformity seen in WT animals (Fig. 3.6). The oscillations in the homozygous tracing are clearly disturbed and these animals also did not show a maximal response even close to that obtained by WT (Fig. 3.9). The disturbed oscillation pattern is most likely to involve GoC, as these cell types are known to express higher levels of CAR8 than GCs and could theoretically be more affected by the mutation. There is a clear dysfunction of the Ca^{2+} signaling in homozygous animals which is due in part to the mutated *Car8* gene; however, this is likely also due to the possible developmental irregularities.

The AUTC results indicate that WT animals experienced an overall increase in Ca^{2+} levels in response to glutamate stimulation, while the mutant groups showed little net change (Fig. 3.10). The fact that WT had a much greater net increase in Ca^{2+} is perplexing since the lack of functional CAR8 in mutants would theoretically cause more intracellular Ca^{2+} release. This result may be due to the general excitatory properties of the bath applied glutamate activating most cell types in the cerebellar cortex. This does show however that general activation caused a net difference in Ca^{2+} response between WT and mutant groups, with the WT group experiencing an increase not seen from mutant groups.

Results of this experiment verifies the hypothesis that all three groups differ significantly in their Ca^{2+} signaling and inclusion of all three groups in subsequent experimental paradigms was required. These findings indicate an over-arching disruption in cerebellar circuitry, likely hampering proper neuronal communication as well as leading to morphological abnormalities.

4.2.2 DHPG Application Experiments

Maximum response results from the analysis of DHPG application were statistically significant (Fig. 3.15). WT animals had a significantly longer time-course than homozygotes and heterozygotes. Average tracings of the GC Ca^{2+} response to DHPG application yielded some interesting qualitative observations. The average tracing from WT animals (Fig. 3.12) shows a modest Ca^{2+} increase in response to DHPG followed by a drop below baseline and possibly establishment on a temporary lower

baseline level for Ca^{2+} homeostasis in the cell. A similar response pattern was observed in the homozygous Ca^{2+} tracing (Fig. 3.14); although, there was a much higher maximal response. The higher maximal response in homozygous animals would be expected. The depression in baseline Ca^{2+} homeostasis may reflect a form of MF-GC LTD, resulting from relatively strong mGluR activation by DHPG [50μM] bath application. There is evidence that activation of group 1 mGluRs leads to LTD of GCs in the hippocampus, a brain region which behaves similarly to the cerebellum with respect to plasticity (Daoudal & Debanne, 2003), through downstream modulation from Ca^{2+} influx (Bortolotto, Fitzjohn, & Collingridge, 1999; Faas et al., 2002). It is unlikely that the drop reflects a loss of viability as the signal seems to begin to recover near the end of the tracings.

AUTC analysis revealed that WT and homozygous animals experienced an overall net depression of Ca^{2+} levels in response to DHPG, while the heterozygous groups showed a net increase (Fig. 3.16). This agrees with the average tracing of heterozygotes (Fig. 3.13) that shows a much longer increase in Ca^{2+} levels than is seen in the other groups. The longer increase in Ca^{2+} levels above baseline seen in heterozygous animals however was not initially expected although has indicated an interesting possibility. The heterozygous increase may be due to the partial knockout of function CAR8 they experience, which would increase intracellular Ca^{2+} signaling. The reason this was not also seen in homozygous animals could be related to their lower number of functional excitatory synapses causing a response similar in magnitude to WT despite problems with CAR8 and intracellular calcium (i.e. a lower number of functional synapses in homozygotes causes a virtual desensitization to excitation).

4.2.3 Electrical Stimulation & AIDA Experiments

Both the glutamate and DHPG bath application experiments yielded useful data; however, there is a lack of external validity since both stimulation paradigms provide a much greater activation than would be encountered *in vivo*. Because of this a set of experiments using electrical stimulation of MFs, which would activate synaptic glutamate receptors via endogenous glutamate release onto GCs was conducted. These results of these experiments further verify the basic premise of this study that homozygous subjects respond with different Ca^{2+} dynamics than the WT and heterozygous groups to an equivalent stimulus.

Slices were stimulated at two time-points during recording to see if plasticity of the MF-GC synapses would be induced with this paradigm. Both the heterozygous and homozygous groups had a lower maximum response of their second peak when compared with the first (Figs. 3.22). The opposite relationship was observed in WT group which had an increase in Ca^{2+} response during the second stimulation. The changes in maximal response seen may be due to either Ca^{2+} store depletion or a form of short-term plasticity. A form of plasticity taking place is quite probable as the stimulation paradigm chosen has previously been reported to induce either LTD or LTP in cerebellar GCs dependent on differential $[Ca^{2+}]_i$ (Bianchi et al., 1992; Gall et al., 2005). Therefore, the conflicting bi-directionality of the change in Ca^{2+} response seen between WT and *wdl* groups likely reflects a difference in basal $[Ca^{2+}]_i$ caused by the mutation. Changes in plasticity within the GCL would heavily alter the information processing capabilities of the cerebellum, as

a large portion of afferent cerebellar information is transmitted and initially processed here.

To further characterize the calcium response observed under the electrical stimulation protocol outlined previously, AIDA bath application was added to the methodology. AIDA is a potent group I mGluR antagonist (Moroni et al., 1997), hence these obtained data allowed a between groups comparison of Ca^{2+} signals generated with and without the contribution of group I mGluRs. Group 1 mGluRs are connected to the IP_3 signaling pathway in GCs which is the pathway hypothesized to be aberrant in *wdl* mice. By antagonizing the group 1 mGluRs we could determine if the Ca^{2+} response of GCs to an *in vivo* like stimulus would be similar between groups when the contribution of IP_3 pathway was inhibited. There was an average drop of approximately 27% in the synaptically induced Ca^{2+} response of all GCs examined with AIDA application which was similar between all groups. This indicates that the group I mGluRs are responsible for about 27% of the somatic GC free Ca^{2+} generated by excitatory activity at the MF-GC synapse (Fig. 3.26). Because there was little difference in the Ca^{2+} response between groups in response to two electrical stimulations in the presence of AIDA and that the same stimulation pattern without AIDA did produced observable differences between groups, it can be deduced that the group 1 mGluRs and their intracellular signaling cascade are what is altered in *wdl* mutants and is leading to the altered Ca^{2+} responses. The involvement of group I mGluRs in intracellular Ca^{2+} release also links their proper function with regular motor learning.

4.2.4 Control Conditions & Experiments

As with any well designed experiment several controls were included in this study to help minimize the influence of inherent variability from the mouse model and variable slice quality. The WT group is considered a control group in this experiment as they do not display any atypical phenotype and have not been manipulated. However, Jackson Labs, the origin point for the *wdl* mice, recommends heterozygous *wdl* mutants as a control group since they do not display the ataxic phenotype (Harris et al., 2003). Both groups were included in these experiments as heterozygotes would still theoretically lack approximately half of the functional CAR8 protein seen in non-mutant wild types and this could still be altering Ca^{2+} homeostasis even if no phenotype is present.

Baseline recordings were conducted at the beginning of each slice being imaged to ensure cells could maintain a steady baseline of Ca^{2+}, an indicator that the cells are still viable after the slicing procedure. If neurons are compromised and essentially "dying", their Ca^{2+} homeostasis is disturbed and Ca^{2+} levels tend to either increase or decrease steadily as opposed to maintain a consistent baseline (Orrenius, Zhivotovsky, & Nicotera, 2003). The dysregulation in Ca^{2+} homeostasis reflects either a failure or overwhelming of mechanisms essential for cell survival such as plasma membrane Ca^{2+} -ATPase pumps (Ivannikov, Sugimori, & Llinás, 2010) or mitochondrial Ca^{2+} sequestration (Gunter et al., 1994). If a slice was unable to maintain a stable baseline level of Ca^{2+} it was not included in the results as this would reflect a lack of slice viability.

In order to ensure the particular experimental condition (i.e. agonist/antagonist application) being employed did not affect the neurons' ability to generate a Ca^{2+} signal,

an additional control test was conducted after recordings. Artificial cerebrospinal fluid (aCSF) with a high concentration of KCl [50mM] (Beani et al., 1994; all other ionic concentrations as specified in methods) was washed into the bath after experimental recordings were complete. The high concentration of KCl causes neurons to depolarize and allows extracellular Ca^{2+} influx to the cell soma; this is a widely utilized method to study Ca^{2+} influx in neuronal cells (Toescu, 1999). In theory, if the experimental condition significantly affected cell viability then we would not see a clear rise in intracellular Ca^{2+} when they were depolarized with high KCl concentration aCSF. There were no slices in this study excluded based on these tests as they all displayed an adequate Ca^{2+} response.

As an additional measure of control to ensure cells remained viable after experimental conditions, propidium iodide (PI) was washed into the bath at the end of several recording sessions for each condition (excluding glutamate experiments). When a slice is exposed to PI the nuclear material of cells is stained when PI enters through pours formed in a cells' plasma membrane with a lack of integrity (Yeh et al., 1981). An image of the area of slice recorded from was taken at the end of the experiment and subsequently PI was washed into the bath followed by another image upon changing the light source filter settings (Fig. 3.5). The two images were then overlaid to determine if cells that took up PI, which would presumably have their viability compromised, also had taken up the Ca^{2+} indicator. It appears that cells which took up PI did not show fluorescence for OG-BAPTA-1-AM and conversely, those cells which showed fluorescence for OG-BAPTA-1-AM did not for PI (Fig. 3.5). This was an ideal result, as it indicates that cells which would be imaged for their Ca^{2+} signaling were viable, as the

cells which were not viable and had taken up PI did not show OG-BAPTA-1-AM fluorescence.

Although no overlap of strong staining of PI and OG-BAPTA-1-AM was observed, there were cells with overlapping with weak staining. This may have been due to non-specific binding of PI to the glass coverslip (Molecular Probes, 1999); however, it cannot be ruled out that some cells that had Ca^{2+} indicator were not viable.

4.2.5 Calcium Imaging Experimental Limitations

Like any experimental methodology, there are inherent limitations to Ca^{2+} imaging which need to be discussed. One of the major contributors of limitations with this methodology is the choice of fluorescent Ca^{2+} probe to be used. Depending on the dissociation constant of a given probe it may be more suited for either determining the time course of a Ca^{2+} signal or give an accurate reading of calcium levels. Probes which dissociate more easily from Ca^{2+}, such as OG-BAPTA-1-AM, are better for determining signal dynamics since they allow for an accurate reading of both the rise and decay phase of a calcium peak. Those probes which do not dissociate from Ca^{2+} easily give a more accurate estimate of absolute calcium levels, but since they bind strongly to Ca^{2+} will not dissociate quickly enough to accurately indicate the decay phase of a signal (Grienberger & Konnerth, 2012).

While analyzing responses from granule cells in several conditions, there was a large amount of variability in their responses to various agonists/antagonists. This may be due to an inherent large variability in granule cell morphology, which was recently

determined to affect signaling through computer modeling (Houston, Wisden, & Brickley, 2012). The authors observed three distinct morphological arrangements of GCs, specifically localization of the axon, which gave three distinct signals when stimulated. This finding explains why there was some significant variability between GCs and also indicates the GC population may be more diverse than previously thought.

4.3 CAR8, Calcium, and Development

CAR8 is first expressed on day 9.5 of the gestational period in mouse embryos in the neuroepithelium (Lakkis et al., 1997) suggesting that it could be involved with pre-natal neuronal development (Aspatwar et al., 2010). Since cerebellar development continues into the first 30 days after birth for mice (Ito, 2006), the effect of CAR8 is having on development could continue into post-natal ages. This hypothesis was supported by the rota-rod data gathered during this project. The homozygous *wdl* mutants started at a disadvantage on the rota-rod compared to other groups and their performance worsens significantly after the first month of life (Fig. 3.3).

Remarkably, a similar ataxic syndrome is seen in humans with a mutation to a gene which is homologues to the murine *Car8*, *CA8* (Türkmen et al., 2009). The CAR8 protein is heavily conserved through various species and maintains a similar expression profile in humans (Aspatwar et al., 2010). Humans who suffer from the *CA8* mutation experience ataxia, mild mental retardation, and quadrapedal gait (Türkmen et al., 2009). Insights gained from the study of the *wdl* mutant could eventually be applied to provide relief from this condition in humans and indirectly add to the growing body of research

surrounding cerebellar based ataxias. Future studies of the *wdl* mouse could include the Morris water maze as a behavioral assay, since it tests both motor functions (i.e. the swimming itself) as well as cognitive aspects (i.e. spatial memory necessary to locate submerged platform).

The developmental dysfunction seen in *wdl* mutants is almost certainly linked to the altered Ca^{2+} signaling. Differential Ca^{2+} concentrations in the developing cerebellar cortex are known to control parallel fibre and climbing fibre innervation. There is ample research that implicates abnormal cerebellar cortex formation in the phenotypic ataxia of various ataxic mouse models (Rhyu, 1999; Hirasawa et al., 2007; Zanjani, 2012). In all of these cases there are structural alterations of the PF-PC synapse which has recently been postulated to encode motor learning (Winter, Li, & Raymond, 2012). These structural alterations are thought to be driven by differential Ca^{2+} concentrations and glutamatergic neurotransmission in the cerebellar cortex during development (Ichikawa et al., 2002; Miyazaki et al., 2004; Takeuchi et al., 2005); both of which were found to be disturbed in the *wdl* mouse (Hirasawa et al., 2007). It is important to keep in mind however, that we cannot rule out the possibility of a yet undiscovered functional role, outside of the IP3R, for CAR8 underlying the aberrant phenotype.

There is an additional role not yet discussed that Ca^{2+} may play in the *wdl* pathology. This involves the fact that Ca^{2+} is known to affect and principally drive fusion of synaptic vesicles with pre-synaptic membrane for exocytosis (DeLorenzo & Freedman, 1978). Gene array studies in the cerebella of *wdl* mice indicate alterations in clusters of genes responsible for vesicle assembly, vesicle transport, signal transduction, and synaptogenesis (Yan et al., 2007). The substantial number of dysregulated genes in *wdl*

mice indicates that CAR8 indeed plays an important physiological role in the cerebellar cortex.

It was interesting that in some analyses the heterozygous animal displayed properties of their GC Ca^{2+} signal that were significantly different from both WT and homozygous animals. This finding was unexpected as heterozygous mutants are normally used as a control in experiments involving *wdl* mice as they display no ataxia. These relatively unexpected findings may be indicative of a biphasic effect which is exerted by CAR8 on intracellular Ca^{2+} dynamics. It is possible that heterozygous animals with only one functional copy of the gene experience Ca^{2+} signaling which is significantly different than WT animals. Homozygous animals therefore have their Ca^{2+} homeostasis disturbed further due to both copies of the *Car8* genes being non-functional, and this initiates a compensatory mechanism (e.g. capacitive Ca^{2+} influx via TRPC channels) causing their signaling to appear similar to WT animals. This phenomenon may also be related to a lower number of functional synapses formed in the ML of homozygous animals (Hirasawa et al., 2007); having an effect on granule cells via a lack of activity at non-functional PF-PC synapses. This would indicate that altered Ca^{2+} signaling may not directly cause the motor deficit by altering neurotransmission; especially since altered Ca^{2+} signaling in GCs is thought to affect motor learning, not cause ataxia (Schonewille et al., 2007) But, may be indirectly causing the ataxia by affecting proper development of the cortex and synapses in homozygous animals.

4.4 Conclusion

Wdl mice show a pronounced ataxia due to a lack of CAR8 expression in the cerebellum leading to aberrant synaptic morphology and significantly altered Ca^{2+} signaling. Previous studies indicated the morphology of excitatory synapses was affected, but that there were likely other factors contributing to ataxia (Hirasawa, 2007). This other factor is likely an effect on Ca^{2+} dynamics. My results have shown significant differences in Ca^{2+} signal dynamics between the GCs of homozygous and heterozygous *wdl* mice as well as WT animals in various stimulation conditions that would activate glutamate receptors. These differences in signaling also likely underlie the previously reported developmental abnormalities as Ca^{2+} is known to be heavily involved in cerebellar cortex development (Zanjani, 2012). Behavioral data indicated that very young *wdl* mice display a significantly less severe ataxic phenotype and show motor learning, which was not seen in *wdl* mice over one month PNA. There was also a lack of motor learning displayed by heterozygous animals over the five days of trials; as was expected there was learning in WT mice. A report by Schonewille et al., 2007, indicated disturbed Ca^{2+} signaling in the cerebellum affected motor learning, no motor performance. Therefore, the fact that both mutant groups (particularly older animals) failed to consistently display motor learning, could be due to the disturbed Ca^{2+} signaling. It may be that the reason heterozygous animals do not display ataxia is that their disturbance in CAR8 functionality is not so severe as to affect earlier cerebellar development. It seems that CAR8 dysfunction could affect development of the GCL as it is expressed at its highest levels during pre-natal maturation (Aspatwar et al., 2010). The underlying issue with homozygous animals then

may not be the originally proposed difference in Ca^{2+} dynamics, but morphological abnormalities in the cerebellar cortex. Continuation of this research line will produce important information regarding the mechanisms of CAR8 function in the cerebellum, and will aid, specifically, in determining the cause of the altered cellular physiology producing ataxia in *wdl* mice.

References

Aizenman, C., & Linden, D. 1999. Regulation of the rebound depolarization and spontaneous firing patterns of deep nuclear neurons in slices of rat cerebellum. *Journal of Neurophysiology*, 82(4), 1697-1709.

Albus, J., 1971. A theory of cerebellar function. *Mathematical Bioscience,* 10, 25–61.

Aspatwar, A., Tolvanen, M.E.E., Ortutay, C., & Parkkila, S., 2010. Carbonic anhydrase related protein VIII and its role in neurodegeneration and cancer. *Current Pharmaceutical Design*, 16, 3264-3276.

Baba, A., Yasui, T., Fujisawa, S., Yamada, R., Yamada, M., Nishiyama, N., & Ikegaya, Y. 2003. Activity-evoked capacitative Ca^{2+} entry: implications in synaptic plasticity. *Journal of Neuroscience*, 23(21), 7737-7741.

Barbour, B., Brunel, N., Hakim, V., & Nadal, J. 2007. What can we learn from synaptic weight distributions? *Trends in Neurosciences*, 30(12), 622-629.

Barmack, N., & Yakhnista, V. 2003. Cerebellar climbing fibres modulate simple spikes in Purkinje cells. *Journal of Neuroscience*, 23(21), 7904-7916.

Beani, L., Tomasini, C., Govoni, B., & Bianchi, C. 1994. Fluorimetric determination of electrically evoked increase in intracellular calcium in cultured cerebellar granule cells. *Journal of Neuroscience Methods*, 51(1), 1-7.

Bianchi, C., Beani, L., Antonelli, T., Vedovato, M., Calo, G., & Tomasini, C. 1992. A simple method for electrical field stimulation of cultured granule cells. *Journal of Neuroscience Methods*, 45(3), 175-182.

Bliss, T., & Collingridge G. 1993. A synaptic model of memory: long-term potentiation in the hippocampus. *Nature*, 361(6407), 31-39.

Bortolotto, Z., Fitzjohn, S., & Collingridge, G. 1999. Roles of metabotropic glutamate receptors in LTP and LTD in. *Current Opinion in Neurobiology*, 9(3), 299-304.

Bruno, R., & Sakmann, B. 2006. Cortex is driven by weak but synchronously active thalamocortical synapses. *Science*, 312(5780), 1622-1627.

Bruno, V., Copani, A., Knöpfel, T., Kuhn, R., Casabona, G., Dell'Albani, P., & Nicoletti, F. 1995. Activation of metabotropic glutamate receptors coupled to inositol phospholipid hydrolysis amplifies NMDA-induced neuronal degeneration in cultured cortical cells. *Neuropharmacology*, 34(8), 1089-1098.

Carter, A., & Regehr, W. 2002. Quantal events shape cerebellar interneuron firing. *Nature Neuroscience*, 5(12), 1309-1318.

Chadderton, P., Margrie, T., & Häusser, M. 2004. Integration of quanta in cerebellar granule cells during sensory processing. *Nature*, 428(6985), 856-860.

Chuquet, J., Hollender, L., & Nimchinsky, E. 2007. High-resolution in vivo imaging of the neurovascular unit during spreading depression. *Journal of Neuroscience*, *27*(15), 4036-4044.

Collingridge, G., & Singer, W. 1990. Excitatory amino acid receptors and synaptic plasticity. *Trends in Pharmacological Sciences*, 11(7), 290-296.

Coesmans, M., Weber, J., De Zeeuw, C., & Hansel, C. 2004. Bidirectional parallel fiber plasticity in the cerebellum under climbing fiber control. *Neuron*, 44(4), 691-700.

Conn, P., & Pin, J. 1997. Pharmacology and functions of metabotropic glutamate receptors. *Annual Review of Pharmacology and Toxicology*, 37(1), 205-237.

Coutinho, V., & Knöpfel, T. 2002. Metabotropic glutamate receptors: electrical and chemical signaling properties. *The Neuroscientist*, 8(6), 551-561.

D'Angelo, E., Rossi, P., Armano, S., & Taglietti, V. 1999. Evidence for NMDA and mGlu receptor-dependent long-term potentiation of mossy fiber–granule cell transmission in rat cerebellum. *Journal of Neurophysiology*, 81(1), 277-287.

D'Angelo, E. 2008. The critical role of Golgi cells in regulating spatio-temporal integration and plasticity at the cerebellum input stage. *Frontiers in Neuroscience*, 2(1), 35.

D'Angelo, E., & De Zeeuw, C. 2008. Timing and plasticity in the cerebellum: focus on the granular layer. *Trends in Neurosciences*, 32(1), 30-40.

Daniel, H., Levenes, C., & Crépel, F. 1998. Cellular mechanisms of cerebellar LTD. *Trends in Neurosciences*, 21(9), 401-406.

Daoudal, G., & Debanne, D. 2003. Long-term plasticity of intrinsic excitability: learning rules and mechanisms. *Learning & Memory*, 10(6), 456-465.

Dawitz, J., Kroon, T., Hjorth, J., & Meredith, R. 2011. Functional calcium imaging in developing cortical networks. *Journal of Visualized Experiments*, 56.

Dean, P., & Porrill, J. 2010. The cerebellum as an adaptive filter: a general model? *Functional Neurology*, 25(3), 173-180.

DeLorenzo, R., & Freedman, S. 1978. Calcium dependent neurotransmitter release and protein phosphorylation in synaptic vesicles. *Biochemical and Biophysical Research Communications*, 80(1), 183-192.

DeZeeuw, C., & Berrebi, A. 1995. Postsynaptic targets of Purkinje cell terminals in the cerebellar and vestibular nuclei of the rat. *European Journal of Neuroscience*, 7, 2322-2333.

DeZeeuw, C., & Yeo, C. 2005. Time and tide in cerebellar memory formation. *Current Opinion in Neurobiology*, 15, 667-674.

Diener, H., & Dichgans, J. 1992. Pathophysiology of cerebellar ataxia. *Movement Disorders*, 7(2), 95-109.

Dieudonné, S. 2004. Submillisecond kinetics and low efficacy of parallel fibre-Golgi cell synaptic currents in the rat cerebellum. *Journal of Physiology*, 510(3), 845-866.

Dodgson, S., Tashian, R., Gross, G., & Carter, N. 1991. The carbonic anhydrases: cellular physiology and molecular genetics. Springer-Plenum, New York.

Draski, L., Nash, D., & Gerhardt, G. 1994. CNS monoamine levels and motoric behaviors in the hotfoot ataxic mutant. *Brain Research*, 645(1), 69-77.

Dugué, G., Brunel, N., Hakim, V., Schwartz, E., Chat, M., Lévesque, M., & Dieudonné, S. 2009. Electrical coupling mediates tunable low-frequency oscillations and resonance in the cerebellar Golgi cell network. *Neuron*, 61(1), 126-139.

Eccles, J.C., Ito, M., & Szentágothai, J. 1967. The Cerebellum as a Neuronal Machine. Springer-Verlag, Berlin.

Eilers. J., Augustine, G., & Konnerth, A. 1995. Subthreshold synaptic Ca^{2+} signaling in fine dendrites and spines of cerebellar Purkinje neurons. *Nature,* 373, 155-158.

Empson, R., & Knopfel, T. 2010. Functional integration of calcium regulatory mechanisms at Purkinje neuron synapses. *Cerebellum*, 11(3), 640-650.

Faas, G., Adwanikar, H., Gereau I., & Saggau, P. 2002. Modulation of presynaptic calcium transients by metabotropic glutamate receptor activation: a differential role in acute depression of synaptic transmission and long-term depression. *Journal of Neuroscience*, 22(16), 6885-6890.

Finch, E., & Augustine, G. 1998. Local calcium signalling by inositol-1,4,5 trisphosphate in Purkinje cell dendrites. *Nature*, 396, 753-756.

Gall, D., Prestori, F., Sola, E., D'Errico, A., Roussel, C., Forti, L., & D'Angelo, E. 2005. Intracellular calcium regulation by burst discharge determines bidirectional long-

term synaptic plasticity at the cerebellum input stage. *Journal of Neuroscience*, 25(19), 4813-4822.

Garwicz, M. 2002. Spinal reflexes provide motor error signals to cerebellar modules—relevance for motor coordination. *Brain Research Reviews*, 40(1-3), 152-165.

Gentet, L., Avermann, M., Matyas, F., Staiger, J., & Petersen, C. (2010). Membrane potential dynamics of GABAergic neurons in the barrel cortex of behaving mice. *Neuron*, 65(3), 422-435.

Grienberger, C., & Konnerth, A. 2012. Imaging calcium in neurons. *Neuron*, 73(5), 862-885.

Gunter, T., Gunter, K., Sheu, S., & Gavin, C. 1994. Mitochondrial calcium transport: physiological and pathological relevance. *American Journal of Physiology-Cell Physiology*, 267(2), C313-C339.

Hansel, C., Artola, A., & Singer, W. 1997. Relation between dendritic Ca^{2+} levels and the polarity of synaptic long-term modification in the rat visual cortex neurons. *European Journal of Neuroscience*, 9, 2309-2322.

Hansel, C. & Linden, D. 2000. Long-term depression of the cerebellar climbing fibre-Purkinje neuron synapse. *Neuron*, 26, 239-247.

Hansel, C., Linden, D., & D Angelo, E. 2001. Beyond parallel fiber LTD: the diversity of synaptic and non-synaptic plasticity in the cerebellum. *Nature Neuroscience*, 4, 467-476.

Harris, B., Ward-Bailey, P., Johnson, K., Bronson, R., & Davisson, M. 2003. A new mutation, waddles (wdl), on mouse Chromosome 4. Mouse Mutant Resources Web Site. The Jackson Laboratory: Bar Harbor, Maine. MGI Direct Data Submission.

Hesslow, G. 1994. Inhibition of classically conditioned eyeblink responses by stimulation of the cerebellar cortex in the decerebrate cat. *Journal of Physiology*, 476(2), 245-256.

Hirawsawa, M., Xu, X., Trask, R., Maddatu, T., Johnson, B., Nagget, J., Nishina, P., & Ikeda, A., 2007. Carbonic anhydrase related protein 8 mutation results in aberrant synaptic morphology and excitatory synaptic function in the cerebellum. *Molecular and Cellular Neuroscience*, 35, 161-170.

Hirota, J., Ando, H., Hamada, K., & Mikoshiba, K., 2003. Carbonic anhydrase-related protein is a novel binding protein for inositol 1,4,5-trisphosphate receptor type 1. *Journal of Biochemistry*, 372, 435-441.

Houston, C., Wisden, W., & Brickley, S. 2012. Axon location determines the input selectivity of cerebellar granule cells. *2012 Neuroscience Meeting Planner*. New Orleans, LA: Society for Neuroscience. Program No. 648.17. Online.

Ichikawa, R., Miyazaki, T., Kano, M., Hashikawa, T., Tatsumi, H., Sakimura, K., & Watanabe, M. 2002. Distal extension of climbing fiber territory and multiple innervation caused by aberrant wiring to adjacent spiny branchlets in cerebellar

Purkinje cells lacking glutamate receptor δ2. *Journal of Neuroscience*, 22(19), 8487-8503.

Ito, M., Kano, M., 1982. Long-lasting depression of parallel fibre-Purkinje cell transmission induced by conjunctive stimulation of parallel fibres and climbing fibres in the cerebellar cortex. *Neuroscience Letters*, 33(3), 253–258.

Ito, M. 2006. Cerebellar circuitry as a neuronal machine. *Progress in Neurobiology,* 78, 272-303.

Ivannikov, M., Sugimori, M., & Llinás, R. 2010. Calcium clearance and its energy requirements in cerebellar neurons. *Cell Calcium*, 47(6), 507-513.

Jakab, R., & Hamori, J. 1988. Quantitative morphology and synaptology of cerebellar glomeruli in the rat. *Anatomy and Embryology*, 179(1), 81-88.

Jiao, Y., Yan, J., Zhao, Y., Donahue, L.R., Beamer, W.G., Li, X., Roe, B.A., Ledoux, M.S., & Gu, W., 2005. Carbonic anhydrase-related protein VIII deficiency is associated with a distinctive lifelong gait disorder in waddles mice. *Genetics*, 171, 1239-1246.

Jones, B. J., & Roberts, D.J. 1968. The quantitative measurement of motor inco-ordination in naïve mice using an accelerating rotarod. *Journal of Pharmacy and Pharmacology*, 20, 302-304.

Jones, K., & Senft, J. 1985. An improved method to determine cell viability by simultaneous staining with fluorescein diacetate-propidium iodide. *Journal of Histochemistry & Cytochemistry*, 33(1), 77-79.

Jörntell, H., & Ekerot, C. 2003. Receptive field plasticity profoundly alters the cutaneous parallel fiber synaptic input to cerebellar interneurons in vivo. *Journal of Neuroscience*, 23(29), 9620-9631.

Jörntell, H., Bengtsson, F., Schonewille, M., & De Zeeuw, C. 2010. Cerebellar molecular layer interneurons–computational properties and roles in learning. *Trends in Neurosciences*, *33*(11), 524-532.

Kandel, E., Schwartz, J., & Jessell, T. (Eds.). 2000. *Principles of Neural Science,* Vol. 4, pp. 837-840. New York: McGraw-Hill.

Kano, M., Kano, M., Fukunaga, K., & Konnerth, A. 1996. Ca^{2+}-induced rebound potentiation of γ-aminobutyric acid-mediated currents requires activation of Ca^{2+}/calmodulin-dependent kinase II. *Proceedings of the National Academy of Sciences*, 93(23), 13351-13356.

Kim, S., Kim, Y., Yuan, J., Petralia, R., Worley, P., Linden, D., 2003. Activation of the TRPC1 cation channel by metabotropic glutamate receptor mGluR1. *Nature*, 426, 285–291.

Kohda, K., Inoue, T, & Mikoshiba, K. 1995. Ca^{2+} release from Ca^{2+} stores, particularly from ryanodine-sensitive Ca^{2+} stores, is required for the induction of LTD in

cultured cerebellar Purkinje cells. *Journal of Neurophysiology*, 74(5), 2184-2188.

Kullmann, D., & Lamsa, K. 2007. Long-term synaptic plasticity in hippocampal interneurons. *Nature Reviews Neuroscience*, 8(9), 687-699.

Kurihara, H., Hashimoto, K., Kano, M., Takayama, C., Sakimura, K., Mishina, M., & Watanabe, M. 1997. Impaired parallel fiber→ Purkinje cell synapse stabilization during cerebellar development of mutant mice lacking the glutamate receptor δ2 subunit. *Journal of Neuroscience*, 17(24), 9613-9623.

Lakkis, M., O'Shea, K., & Tashian, R. 1997. Differential expression of the carbonic anhydrase genes for CA VII (Car7) and CA-RP VIII (Car8) in mouse brain. *Journal of Histochemistry & Cytochemistry*, 45(5), 657-662.

Lalonde, R., & Strazielle, C. 2001. Motor performance and regional brain metabolism of spontaneous murine mutations with cerebellar atrophy. *Behavioural Brain Research*, 125(1), 103-108.

Lamont, M., & Weber, J. 2012. The role of calcium in synaptic plasticity and motor learning in the cerebellar cortex. *Neuroscience & Biobehavioral Reviews*.

Lev-Ram, V., Wong, S., Storm, D., & Tsien, R. 2002. A new form of cerebellar long-term potentiation is postsynaptic and depends on nitric oxide but not cAMP. *Proceedings of the National Academy of Sciences*, 99(12), 8389-8393.

Liu, S., & Cull-Candy, S. 2000. Synaptic activity at calcium-permeable AMPA receptors induces a switch in receptor subtype. *Nature*, 405(6785), 454-458.

Liu, S., & Cull-Candy, S. 2002. Activity-dependent change in AMPA receptor properties in cerebellar stellate cells. *Journal of Neuroscience*, 22(10), 3881-3889.

Liu, S., & Cull-Candy, S. 2005. Subunit interaction with PICK and GRIP controls Ca^{2+} permeability of AMPARs at cerebellar synapses. *Nature Neuroscience*, 8(6), 768-775.

Llano, I., Dreessen, J., Kano, M., Konnerth, A. 1991. Intradendritic release of calcium induced by glutamate in cerebellar Purkinje cells. *Neuron*, 7, 577–583.

Lorez, M., Humbel, U., Pflimlin, M., & Kew, J. 2009. Group III metabotropic glutamate receptors as autoreceptors in the cerebellar cortex. *British Journal of Pharmacology*, 138(4), 614-625.

Lu, H., Hartmann, M., & Bower, J. 2005. Correlations between purkinje cell single-unit activity and simultaneously recorded field potentials in the immediately underlying granule cell layer. *Journal of Neurophysiology*, 94, 1849-1860.

Ma, H., Patterson, R., van Rossum, D., Birnbaumer, L., Mikoshiba, K., Gill, D. 2000. Requirement of the inositol trisphosphate receptor for activation of store-operated Ca^{2+} channels. *Science*, 287, 1647–1651.

Malenka, R., & Nicoll, R. 1999. Long-term potentiation – a decade of progress? *Science*, 285, 1870-1874.

Mandolesi, G., Autuori, E., Cesa, R., Premoselli, F., Cesare, P., & Strata, P. 2009. GluRδ2 expression in the mature cerebellum of hotfoot mice promotes parallel fiber synaptogenesis and axonal competition. *Public Library of Science ONE*, 4(4), e5243.

Mann-Metzer, P., & Yarom, Y. 1999. Electrotonic coupling interacts with intrinsic properties to generate synchronized activity in cerebellar networks of inhibitory interneurons. *The Journal of Neuroscience*, 19(9), 3298-3306.

Manto, M., & Jissendi, P. 2012. Cerebellum: links between development, developmental disorders and motor learning. *Frontiers in Neuroanatomy*, 6, 1.

Marr, D. 1969. A theory of cerebellar cortex. *Journal of Physiology*, 202(2), 437-470.

Massey, P., & Bashir, Z. 2007. Long-term depression: multiple forms and implications for brain function. *Trends in Neurosciences*, 30(4), 176-184.

Medina, J., Nores, W., Mauk, M., 2002. Inhibition of climbing fibres is a signal for the extinction of conditioned eyelid responses. *Nature*, 416(6878), 330–333.

Mitchell, S., & Silver, R. 2000. GABA spillover from single inhibitory axons suppresses low-frequency excitatory transmission at the cerebellar glomerulus. *Journal of Neuroscience*, 20(23), 8651-8658.

Mittmann, W., & Häusser, M. 2007. Linking synaptic plasticity and spike output at excitatory and inhibitory synapses onto cerebellar Purkinje cells. *Journal of Neuroscience*, 27(21), 5559-5570.

Miyazaki, T., Hashimoto, K., Shin, H.S., Kano, M., Watanabe, M., 2004. P/Q-type Ca2+ channel alpha1A regulates synaptic competition on developing cerebellar Purkinje cells. *Journal of Neuroscience*, 24(7), 1734-1743.

Molecular Probes. 1999. *Propidium iodide nucleic acid stain.* Retrieved from http://www.cbm.uam.es/confocal/Manuales/Ioduro%20propidio.pdf

Monville, C., Torres, E., & Dunnett, S. 2006. Comparison of incremental and accelerating protocols of the rotarod test for the assessment of motor deficits in the 6-OHDA model. *Journal of Neuroscience Methods*, 158(2), 219-223.

Moroni, F., Lombardi, G., Thomsen, C., Leonardi, P., Attucci, S., Peruginelli, F., Torregrossa, S., Pellegrini-Giampiettro, D., Luneia, R., & Pelliccian, R. 1997. Pharmacological characterization of 1-aminoindan-1,5-dicarboxylic acid, a potent mGluR1 antagonist. *Journal of Pharmacology and Experimental Therapeutics*, 281(2), 721-729.

Morris, R. 1989. Synaptic plasticity and learning: selective impairment of learning rats and blockade of long-term potentiation in vivo by the N-methyl-D-aspartate receptor antagonist AP5. *Journal of Neuroscience*, 9(9), 3040-3057.

Mulkey, R., Malenka, R. 1992. Mechanisms underlying induction of homosynaptic long-term depression in area CA1 of the hippocampus. *Neuron*, 9, 967-975.

Nieus, T., Sola, E., Mapelli, J., Saftenku, E., Rossi, P., & D'angelo, E. 2006. LTP regulates burst initiation and frequency at mossy fiber–granule cell synapses of

rat cerebellum: experimental observations and theoretical predictions. *Journal of Neurophysiology*, 95(2), 686-699.

Okubo, Y., Kakizawa, S., Hirose, K., & Iino, M., 2001. Visualization of IP3 dynamics reveals a novel AMPA receptor-triggered IP3 production pathway mediated by voltage-dependent Ca^{2+} influx in Purkinje cells. *Neuron*, 32, 113–122.

Orrenius, S., Zhivotovsky, B., & Nicotera, P. 2003. Regulation of cell death: the calcium–apoptosis link. *Nature Reviews Molecular Cell Biology*, 4(7), 552-565.

Otani, S., Daniel, H., Takita, M., & Crepel, F. 2002. Long-term depression induced by postsynaptic group II metabotropic glutamate receptors linked to phospholipase C and intracellular calcium rises in rat prefrontal cortex. *Journal of Neuroscience*, 22(9), 3434-3444.

Palkovits, M., Magyar, P., & Szentagothai, J. 1971. Quantitative histological analysis of the cerebellar cortex in the cat: II. Cell numbers and densities in the granular layer. *Brain Research*, 32(1), 15-30.

Pellionisz, A., & Szentágothai, J. 1973. Dynamic single unit simulation of a realistic cerebellar network model. *Brain Research*, 49(1), 83-99.

Piochon, C., Irinopoulou, T., Brusciano, D., Bailly, Y., Mariani, J., & Levenes, C. 2007. NMDA receptor contribution to the climbing fiber response in the adult mouse Purkinje cell. *Journal of Neuroscience*, 27(40), 10797-10809.

Piochon, C., Levenes, C., Ohtsuki, G., Hansel, C. 2010. Purkinje cell NMDA receptors assume a key role in synaptic gain control in the mature cerebellum. *Journal of Neuroscience*, 30(45), 15330-15335.

Pöschel, B., & Manahan-Vaughan, D. 2005. Group II mGluR-induced long term depression in the dentate gyrus in vivo is NMDA receptor-independent and does not require protein synthesis. *Neuropharmacology*, 49, 1-12.

Rahman, S., & Neuman, R. 1996. Characterization of metabotropic glutamate receptor-mediated facilitation of N-methyl-D-aspartate depolarization of neocortical neurones. *British Journal of Pharmacology*, 117(4), 675-683.

Rancillac, A., & Crépel, F. 2004. Synapses between parallel fibres and stellate cells express long-term changes in synaptic efficacy in rat cerebellum. *Journal of Physiology*, 554(3), 707-720.

Randall, A., & Tsien, R. 1995. Pharmacological dissection of multiple types of Ca2+ channel currents in rat cerebellar granule neurons. *Journal of Neuroscience*, 15(4), 2995-3012.

Renzi, M., Farrant, M., & Cull-Candy, S. 2007. Climbing-fibre activation of NMDA receptors in Purkinje cells of adult mice. *Journal of Physiology*, 585(1), 91-101.

Rhyu, I., Abbott, L., Walker, D., & Sotelo, C. 1999. An ultrastructural study of granule cell/Purkinje cell synapses in tottering (tg/tg), leaner (tg^{la}/tg^{la}) and compound heterozygous tottering/leaner (tg/tg^{la}) mice. *Neuroscience*, 90(3), 717-728.

Rinaldo, L., & Hansel, C. 2010. Ataxias and cerebellar dysfunction: involvement of synaptic plasticity deficits?. *Functional Neurology*, 25(3), 135-139.

Robberechts, Q., Wijnants, M., Giugliano, M., & De Schutter, E. 2010. Long-term depression at parallel fiber to Golgi cell synapses. *Journal of Neurophysiology*, 104(6), 3413-3423.

Robinson, M., & Coyle, J. 1987. Glutamate and related acidic excitatory neurotransmitters: from basic science to clinical application. *The FASEB Journal*, 1(6), 446-455.

Rose, C., & Konnerth, A. 2001. Stores not just for storage: intracellular calcium release and synaptic plasticity. *Neuron*, 31(4), 519-522.

Rustay, N., Wahlsten, D., & Crabbe, J. 2003. Influence of task parameters on rotarod performance and sensitivity to ethanol in mice. *Behavioral Brain Research*, 141, 237-249.

Salin, P., Malenka, R., & Nicoll, R. 1996. Cyclic AMP mediates a presynaptic form of LTP at cerebellar parallel fibre synapses. *Neuron*, 16, 797-803.

Sánchez-Campusano, R., Gruart, A., & Delgado-García, J. 2007. The cerebellar interpositus nucleus and the dynamic control of learned motor responses. *The Journal of Neuroscience*, 27(25), 6620-6632.

Schmahmann, J. 2004. Disorders of the cerebellum: ataxia, dysmetria of thought, and the cerebellar cognitive affective syndrome. *Journal of Neuropsychiatry and Clinical Neurosciences*, 16(3), 367-378.

Schmolesky, M., Weber, J., DeZeeuw, C., Hansel, C. 2002. The making of a complex spike: ionic composition and plasticity. *Annals of the New York Academy of Science*, 978, 359-390.

Schonewille, M., Wulf, P., Farrant, M., Wisden, W., & De Zeeuw, C. 2007. Interneurons in the molecular layer of the cerebellum are required for consolidation of motor learning. *2007 Neuroscience Meeting Planner*. San Diego, CA: Society for Neuroscience. Program No. 190.13. Online.

Schonewille, M., Belmeguenai, A., Koekkoek, S., Houtman, S., Boele, H., van Beugen, B., Gao, Z., Badura, A., Ohtsuki, G., Amerika, W., Hosy, E., Hoebeek, F., Elgersma, Y., Hansel, C., & De Zeeuw, C. 2010. Purkinje cell-specific knockout of the protein phosphatase PP2B impairs potentiation and cerebellar motor learning. *Neuron*, 67(4), 618-628.

Scelfo, B., Sacchetti, B., & Strata, P. 2008. Learning-related long-term potentiation of inhibitory synapses in the cerebellar cortex. *Proceedings of the National Academy of Sciences*, 105(2), 769-774.

Sims, R., & Hartell, N. 2006. Differential susceptibility to synaptic plasticity reveals a functional specialization of ascending axon and parallel fiber synapses to cerebellar Purkinje cells. *Journal of Neuroscience*, 26(19), 5153-5159.

Sola, E., Prestori, F., Rossi, P., Taglietti, V., & D'Angelo, E. 2004. Increased neurotransmitter release during long-term potentiation at mossy fibre–granule cell synapses in rat cerebellum. *The Journal of Physiology*, 557(3), 843-861.

Stanton, M., Freeman, J., & Skelton, R. 1992. Eyeblink conditioning in the developing rat. *Behavioral Neuroscience*, 106(4), 657-665.

Stoodley, C., & Schmahmann, J. 2010. Evidence for topographic organization in the cerebellum of motor control versus cognitive and affective processing. *Cortex*, 46(7), 831-844.

Svensson, P., Jirenhed, D., Bengtsson, F., & Hesslow, G. 2010. Effect of conditioned stimulus parameters on timing of conditioned Purkinje cell responses. *Journal of Neurophysiology*, 103(3), 1329-1336.

Szapiro, G., & Barbour, B. 2007. Multiple climbing fibers signal to molecular layer interneurons exclusively via glutamate spillover. *Nature Neuroscience*, 10(6), 735-742.

Tahon, K., Volny-Luraghi, A., & De Schutter, E. 2005. Temporal characteristics of tactile stimuli influence the response profile of cerebellar Golgi cells. *Neuroscience Letters*, 390(3), 156-161.

Takeuchi, T., Miyazaki, T., Watanabe, M., Mori, H., Sakimura, K., & Mishina, M. 2005. Control of synaptic connection by glutamate receptor δ2 in the adult cerebellum. *Journal of Neuroscience*, 25(8), 2146-2156.

Taniuchi, K., Nishimori, I., Takeuchi, T., Fujikawa-Adachi, K., Ohtsuki, Y., & Onishi, S. 2002. Developmental expression of carbonic anhydrase-related proteins VIII, X, and XI in the human brain. *Neuroscience*, 112(1), 93-99.

Thomsen, L., Jörntell, H., & Midtgaard, J. 2010. Presynaptic calcium signalling in cerebellar mossy fibres. *Frontiers in Neural Circuits*, 4, 1-15.

Toescu, E. 1999. Activity of voltage-operated calcium channels in rat cerebellar granule neurons and neuronal survival. *Neuroscience*, 94(2), 561-570.

Türkmen, S., Guo, G., Garshasbi, M., Hoffmann, K., Alshalah, A., Mischung, C., & Robinson, P. 2009. CA8 mutations cause a novel syndrome characterized by ataxia and mild mental retardation with predisposition to quadrupedal gait. *PLoS Genetics*, 5(5), e1000487.

van Kan, P., Gibson, A., & Houk, J. 1993. Movement-related inputs to intermediate cerebellum of the monkey. *Journal of Neurophysiology*, 69(1), 74-94.

Weber, J., Rzigalinski, B., & Ellis, E. 2001. Traumatic injury of cortical neurons causes changes in intracellular calcium stores and capacitative calcium influx. *Journal of Biological Chemistry*, 276(3), 1800-1807.

Weber, J., DeZeeuw, C., Linden, D., & Hansel, C. 2003. Long-term depression of climbing fibre-evoked calcium transients in Purkinje cell dendrites. *Proceedings of the National Academy of Sciences U.S.A.*, 100, 2878-2883.

Wilt, B., Burns, L., Ho, E., Ghosh, K., Mukamel, E., & Schnitzer, M. 2009. Advances in light microscopy for neuroscience. *Annual Review of Neuroscience*, 32, 435.

Winter, O., Li, L., Raymond, J. 2012. Is motor learning encoded by structural alterations in cerebellar parallel fibers? *2012 Neuroscience Meeting Planner*. New Orleans, LA: Society for Neuroscience. Program No. 477.27. Online.

Xu, W., & Edgley, S. 2008. Climbing fibre-dependent changes in Golgi cell responses to peripheral stimulation. *Journal of Physiology*, 586(20), 4951-4959.

Yan, J., Jiao, Y., Jiao, F., Stuart, J., Donahue, L., Beamer, W., & Gu, W. 2007. Effects of carbonic anhydrase VIII deficiency on cerebellar gene expression profiles in the wdl mouse. *Neuroscience Letters*, 413(3), 196-201.

Yeh, C., Hsi, B., & Faulk, W. 1981. Propidium iodide as a nuclear marker in immunofluorescence. II. Use with cellular identification and viability studies. *Journal of Immunological Methods*, 43(3), 269.

Zagha, E., Manita, S., Ross, W., & Rudy, B. 2010. Dendritic $Kv_{3.3}$ potassium channels in cerebellar Purkinje cells regulate generation and spatial dynamics of dendritic Ca2+ spikes. *Journal of Neurophysiology*, 103(6), 3516-3525.

Zanjani, H., Vogel, M., Mariani, J. 2012. Morphometric and quantitative analysis of cerebellar Purkinje and granule cells in the hotfoot ($Grid2^{ho/ho}$) mutant mice. *2012 Neuroscience Meeting Planner*. New Orleans, LA: Society for Neuroscience. Program No. 652.01. Online.

Zhang, W., & Linden, D. 2006. Long-term depression at the mossy fiber–deep cerebellar nucleus synapse. *Journal of Neuroscience*, 26(26), 6935-6944.

Zlomuzica, A., Burghoff, S., Schrader, J., & Dere, E. 2012. Superior working memory and behavioural habituation but diminished psychomotor coordination in mice lacking the ecto-5′-nucleotidase (CD73) gene. *Purinergic signalling*, 1-8.